Carderock Division
Naval Surface Warfare Center
West Bethesda, MD 20817-5700

CARDIVNSWC – TR - 61 – 98 – 21 Sept. 1998

Survivability, Structures, and Materials Directorate
Technical Report

Characterization of the Surface Film Growth During the Electrochemical Process: Part II (90 % Copper – 10 % Nickel System)

by

A. Srinivasa Rao

NSWCCD TR– 61– 98 - 21 Characerization of the Surface Film Growth During the Electrochemical Process: Part II (90 % Copper– 10 % Nickel System)

Carderock Division
Naval Surface Warfare Center
West Bethesda, MD 20817-5700

CARDIVNSWC – TR - 61 – 98 – 21 Sept. 1998

Survivability, Structures, and Materials Directorate Technical Report

Characerization of the Surface Film Growth During the Electrochemical Process: Part II (90 % Copper – 10 % Nickel System)

by

A. Srinivasa Rao

REPORT DOCUMENTATION PAGE

Form Approved
OMB No. 0704-0188

1. AGENCY USE ONLY (Leave blank)	2. REPORT DATE	3. REPORT TYPE AND DATES COVERED
	June 1998	Research and Development

4. TITLE AND SUBTITLE
Characerization of the Surface Film Growth During the Electrochemical Process: Part II 90 % Copper – 10 % Nickel System

5. FUNDING NUMBERS
98-1-6120-600

6. AUTHOR(S)
A. Srinivasa Rao

7. PERFORMING ORGANIZATION NAME(S) AND ADDRESS(ES)
Carderock Division
Naval Surface Warfare Center
Bethesda, MD 20817-5000

8. PERFORMING ORGANIZATION REPORT NUMBER
TR- 61 – 98 - 21

9. SPONSORING/MONITORING AGENCY NAME(S) AND ADDRESS(ES)
Strategic Research Initiative Program
Electric Power Research Institute
Palo Alto, CA

10. SPONSORING/MONITORING AGENCY REPORT NUMBER

11. SUPPLEMENTARY NOTES

12a. DISTRIBUTION/AVAILABILITY STATEMENT
Distribution unlimited. Approved for public release

12b. DISTRIBUTION CODE

In order to understand the resistance of passive films formed during corrosion processes, an analytical technique using x-ray diffraction was developed to examine the structure of metal in closest proximity to the metal / liquid interface. The in-situ structure at the metal liquid interface was examined for 90 % copper and 10 % nickel (90-10 Cu-Ni) in KOH solution at room temperature and at four different potentistatically controlled potentials (-0.5 V, - 0.1 V, + 0.5 V and +0.10 V versus Ni/NiO). The chemical changes at the metal interface were studied over a period of 48 hours. It was found that the integrity of the 90-10 Cu-Ni foil in KOH was lost after a continued application of the potential over 48 hours. The x-ray diffraction results indicated that the structure of both the inner and the outer passive layers, at –0.5V and - 0.1 V (versus Ni/NiO), is comprised of $Ni(OH)_2$, $Cu(OH)_2$, NiOOH and Cu_2O NiO. Similarly the structure of the interfaces at + 0.5 V and + 0.10 V (versus Ni/NiO) contains NiO, Ni_2O_3, Cu_2O NiO and Ni_2CuO_3. XPS analysis of the surface structure (primarily of the outer passive layer) suggests that at - 0.50 V (versus Ni/NiO) the structure consists of $Ni(OH)_2$, $Cu(OH)_2$ and CuO. The structure at +0.50 V (versus Ni/NiO) consists of NiO, Ni_2O_3, $Ni(OH)_2$, $Cu(OH)_2$ and CuO. It is therefore possible that the structure of inner passive layer may be NiOOH at – 0.5 V and - 0.10 V and $Ni(OH)_2$ at + 0.50 V and + 0.1 V.

14. SUBJECT TERMS

15. NUMBER OF PAGES

16. PRICE CODE

17. SECURITY CLASSIFICATION OF REPORT	18. SECURITY CLASSIFICATION OF THIS PAGE	19. SECURITY CLASSIFICATION OF ABSTRACT	20. LIMITATION OF ABSTRACT
Unclassified	Unclassified	Unclassified	Unclassified

CONTENTS

FIGURES

Page No.

Page No.

Page No.

ABSTRACT

In order to understand the resistance of passive films formed during corrosion processes, an analytical technique using x-ray diffraction was developed to examine the structure of metal in closest proximity to the metal / liquid interface. The in-situ structure at the metal liquid interface was examined for 90 % copper and 10 % nickel (90-10 Cu-Ni) in KOH solution at room temperature and at four different potentistatically controlled potentials (-0.5 V, - 0.1 V, + 0.5 V and +0.10 V versus Ni/NiO). The chemical changes at the metal interface were studied over a period of 48 hours. It was found that the integrity of the 90-10 Cu-Ni foil in KOH was lost after a continued application of the potential over 48 hours. The x-ray diffraction results indicated that the structure of both the inner and the outer passive layers, at –0.5V and - 0.1 V (versus Ni/NiO), is comprised of $Ni(OH)_2$, $Cu(OH)_2$, NiOOH and Cu_2O NiO. Similarly the structure of the interfaces at + 0.5 V and + 0.10 V (versus Ni/NiO) contains NiO, Ni_2O_3, Cu_2O NiO and Ni_2CuO_3. XPS analysis of the surface structure (primarily of the outer passive layer) suggests that at - 0.50 V (versus Ni/NiO) the structure consists of $Ni(OH)_2$, $Cu(OH)_2$ and CuO. The structure at +0.50 V (versus Ni/NiO) consists of NiO, Ni_2O_3, $Ni(OH)_2$, $Cu(OH)_2$ and CuO. It is therefore possible that the structure of inner passive layer may be NiOOH at – 0.5 V and - 0.10 V and $Ni(OH)_2$ at + 0.50 V and + 0.1 V.

ADMINSTRATIVE INFORMATION

This project was funded by the Electric Power Research Institute (EPRI), Palo Alto, CA and administered by the Materials Corrosion Program manager, Dr. Larry J. Nelson, under the Strategic Research Initiative Program. The work was performed at the Carderock Division of the Naval Surface Warfare Center (CDNSWC) under the Contract Number: W08041-l0 and Work Unit Number 1-6120-600. This work was supervised Within the Metals Department (Code 61) by Dr. L. F. Aprigliano (Code 612).

INTRODUCTION

BACKGROUND

The development of new materials with improved hot water and salt-water corrosion resistance is very important. As these materials are being proven, it is also important to develop procedures and methods to maintain the existing materials currently in use. Technologically advanced maintenance procedures would have applications in several areas, viz. electric utilities for the removal of deposits from thermal power plant equipment, and in the civilian and military ship building industry for the removal of corrosion products from ship platforms and on-board tanks. Reductions in military and industrial acquisition budgets have led to reduced new equipment purchases. Therefore, the need has increased to extend the operational life of the current systems. In addition, the environmental constraints on materials selection and maintenance processes are increasingly becoming a major concern in utility plant operation and maintenance.

A key to the extension of equipment life is the reduction of material degradation/ failure rates. The degradation rates of both naval and electrical utility systems are exacerbated by salt water and hot corrosion. The lessons learned to control the corrosion in one system can be used to the benefit of another. The use of thin films, e.g. oxides, has been the first line of defense in protecting machinery systems from the onset of corrosion. When these films are passive to the environment, they can impart excellent corrosion resistance. A fundamental, electrochemical understanding of how passive films resist

the effects of corrodants will provide a means to improve the life of machinery components.

Saltwater and hot corrosion processes are controlled by the chemical reactions that take place at the metal/liquid interface. In general, this is often studied with analytical techniques that look through the liquid to see the interface. Although it is more difficult, it may be far more revealing to view this interface by looking at it from the other side - through the metal. By doing this, new information can be gained concerning the manner in which a passive film resists the action of a liquid corrodant. This information can then be used to design more protective films in systems that are not normally passive. The passive film formation process involves the transformation of a metal into a desirable compound. If one is to interrupt this process, it is useful to know if the final compound is preceded by the meaningful formation of an intermediate compound.

In the recent past, a number of in-situ and structure sensitive studies were made of electrochemical processes within the confines of conventional and ultra high vacuum systems (uhv) systems. [1-3]. Most of these earlier studies involved the emission and or the scattering of photons or charged particles as a part of the analysis technique. These techniques could provide only indirect information regarding the structure of the corrosion products and interfaces. In the open literature, there have been reports on the elucidation of structure during electrochemical processing using neutron diffraction [4]. However, the neutron diffraction studies required an elaborate and complex experimental set up. Of late, a few investigators have suggested the feasibility of experiments using

analytical techniques such as the surface extended x-ray adsorption fine structure (SEXAFS), x-ray adsorption near edge structure (XANES), and total external reflection Bragg diffraction (TRBD) [5-8]. However, these studies often ignored the near-metal side of the metal/liquid interface, because the extent of the reaction product is so much broader on the liquid side than the metal side (1-10 μm versus 1-20 nm) of the metal/liquid interface.

NICKEL / NICKEL ALLOY SYSTEM

The electrochemistry of nickel and nickel alloy systems warrants study by the scientific community because these systems are pertinent to many utility and naval machinery components. During corrosion, nickel and its alloys undergo the formation of passive oxyhydrates and/or hydroxides. In the literature it has been reported that the identification of the formation of nickel hydroxides and or oxyhydrates has been difficult because these compounds often have highly disordered and/or have an amorphous crystal structure. Several earlier researchers used analytical techniques such as the EXAFS [5-6] and XAS [7-8] to study nickel compounds. However, these researchers focussed their attention on understanding the oxidation state of the nickel (Ni^{4+}) during the electrochemical process instead of examining the nucleation and growth of new compositions at the interface.

Except for two earlier studies [10,11] that have focussed their attention on understanding the structure of the near metal side of the metal liquid interface, no other reports were cited in the open literature. In one [10], it was reported that the in-situ x-ray

diffraction study is the key to understanding the electrochemical processes at the nickel electrode solution interface. These researchers designed and developed an electrochemical cell for x-ray reflection mode experiments. They reported that they found a 0.75 μm thick layer of $Ni(OH)_2$ after 40 hours of chemical reaction of nickel in 5 M KOH at 1 mV/sec. However, their x-ray diffraction data showed very broad peaks. They concluded that the broadening was due to a mixture of phases in incompletely aged electrodes.

Another in-situ x-ray diffraction analysis [12] involved the study of the structure of nickel electrodes during hydrogen evolution in sulfuric acid electrolysis. Those investigators reported that by x-ray diffraction they observed the formation of β-NiH. They have also reported that they resolved the structure of β-NiH by x-ray diffraction. The peaks were very sharp and the 2θ values corresponding to β-NiH (111),(200) and (220) were at 41.9, 48.8 and 71.1 respectively.

PASSIVE LAYER DEGRADATION

The passive oxide films/ layers on many corrosion resistant alloys (e.g. stainless steels and copper/nickel alloys) are what distinguish them from alloys that readily corrode in aqueous environments. However, even these alloys can corrode and their passive layers degrade in many industrial applications. The mechanism of passive layer degradation has been extensively studied from the perspective of the aqueous side of the process. It has not been extensively studied from the perspective of the metal side of the process, due to the complexity of the interface region. As the electrochemical reaction

starts, at the interface, the metal will be converted to its corresponding oxide. This oxide layer then may act as a passive barrier, thus retarding progression of the electrochemical process. The intriguing question is whether the passive film extends from the solution to the reacting interface of the metal and or whether it forms another transient inner passive layer? Assuming that such a process exists, the electrochemical process can be represented schematically as follows. Figure 1 shows a schematic diagram of the metal - solution interface region during an electrochemical reaction process. The metal interface region can be divided into possibly four regions: (a) bulk metal, (b) inner passive layer, (c) outer passive layer and (d) solution. The existence of an inner passive layer (nano meters (10 - 20 nm) thick) has widely been accepted by the scientific community. Most of the earlier conventional studies have studied the degradation of the passive layers by observing the interface region from the solution side (Figure 1(A)). The proposed, present approach will be to investigate the structure of the inner passive layer from the metal side of the metal solution interface (as shown in Figure 1(B)). The motivation to the present approach is the desire to establish whether the inner passive layer has an epitaxial growth which can make a better passive system and whether such a thin film growth can be detected by the present experimental analytical technique.

OBJECTIVES

The objectives of this research project are to:

1. to develop an analytical method to study from the metal side the corrosion reaction at the metal/liquid interface;

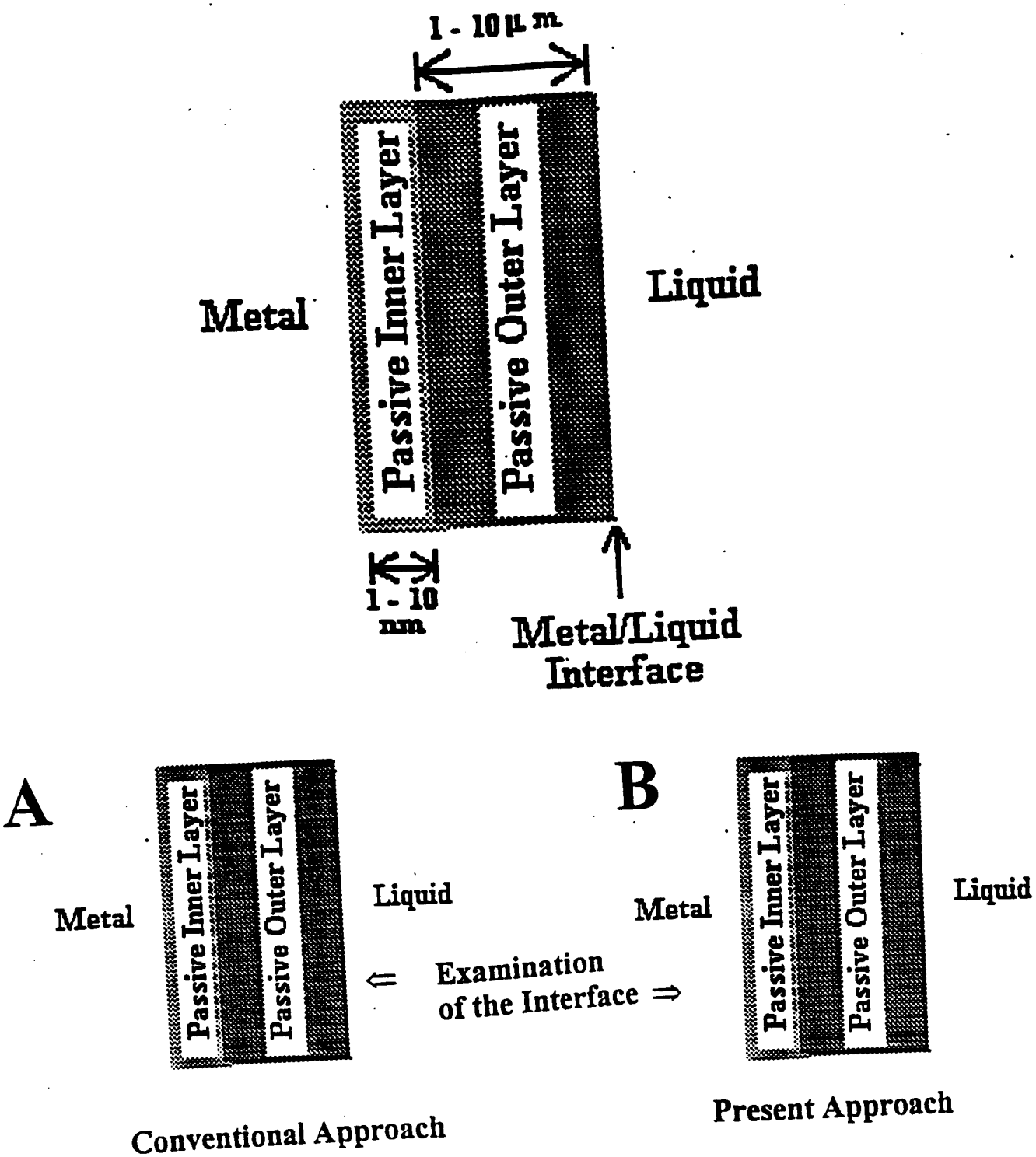

Figure 1. Schematic diagram of the metal/solution interface region during electrochemical reaction process. (A) Conventional and (B) present approach to study the inner passive layer.

2. apply this method to study the reaction at an elemental metal/corrodant interface, i.e. nickel/KOH;

3. apply this method to alloy metal systems, specifically 90/10 and/or 70/30 Cu/Ni.

The work to be reported below details our study of the 90/10 Cu/Ni, KOH reaction.

EXPERIMENTAL PROCEDURE

As part of the first phase of this project an experimental electrochemical cell was designed, fabricated, and tested [13]. This cell was designed to allow for the use of x-ray diffraction as a method to study the corrosion process from the metal side of the metal/liquid interface. In that first phase of our work, the nickel – KOH interface was studied in conjunction with the electrochemical characteristics of the corrosion process in the cell. The details of the cell design and the experimental results on the Ni/KOH system were given in our first project report [13].

MATERIALS

A commercial grade alloy of 90 % copper and 10 % nickel, known as Alloy 725, were procured from the Eagle Brass Company, Leesport, PA. The alloy samples were supplied in a 0.003" thick sheets of Annealed Deep Draw Quality. The chemical

composition and the mechanical properties were:

Chemical Composition :	89.22 % Cu; 8.77 % Ni; 1.94% Sn; 0.002% Fe; 0.020 % Zn and < 0.002% Pb.
Alloy Sheet Thickness After Rolling	~ 0.003"
Tensile Strength	~ 69 –70 ksi
% Elongation	~ 5 – 8 %.
Sheet Quality :	Annealed Deep Draw Quality

The details of the rolling method and procedures to make the sheets were unavailable. The as-procured 90-10 Cu-Ni sheets were cut into 6"x 6" samples, and they were chemically thinned using nitric acid. The samples were placed in a plastic tray containing 1 M nitric acid solution. The tray was gently shaken in order to obtain a uniform thinning. Once the samples were thinned to ~ 0.001" thick, they were cleaned using distilled water and were placed in a second tray containing 0.1 M nitric acid. The sample thinning was continued until the thickness was reduced to 0.0005". The foils were then thoroughly cleaned in distilled water bath in which the water was circulated continuously for 30 minutes. The foils were then air-dried.

ELECTROCHEMICAL CELL DESIGN

Figure 2 shows a schematic diagram of the electrochemical cell. It was designed to be easily attached to and detached from the x-ray unit. A noteworthy feature of this cell design is that the top surface of the electrochemical cell was kept at an inclined angle of 5° to the plane of the x-ray beam. At the mid point of the cell width, the cell surface is

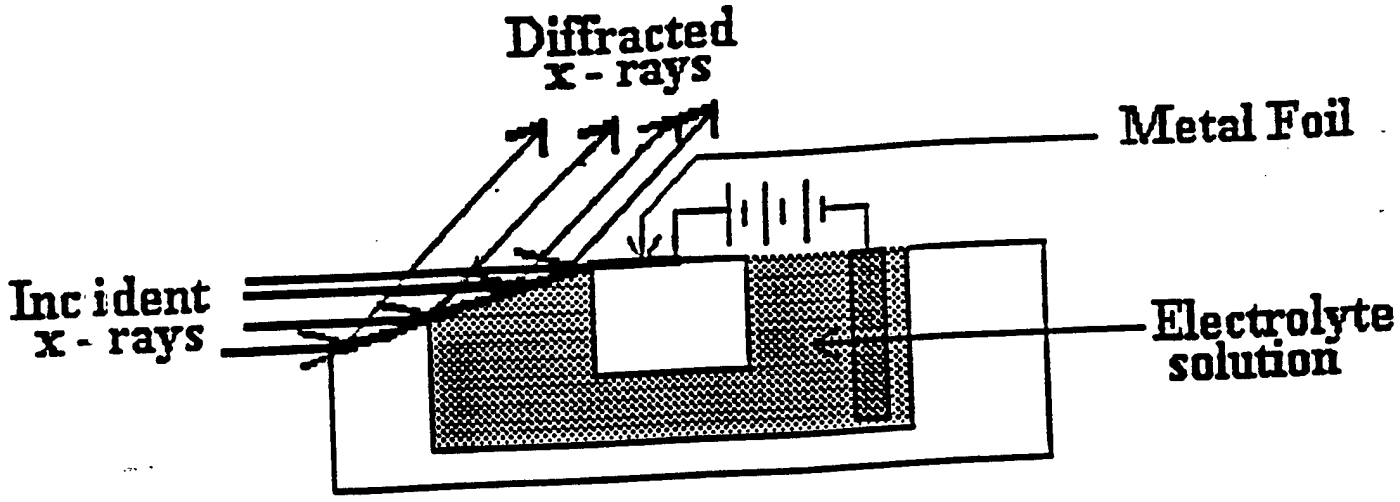

Figure 2. Schematic diagram of the design of the electrochemical cell.

in plane with the incident x-rays The inclination of the cell surface provides for strong and sharp Bragg reflections, thus resolving sharp x-ray peaks. The need for the 5^{o} inclination of the top surface of the cell was discovered by a process of trial and error.

ELECTROCHEMICAL PARAMETERS

In order to establish electrochemical parameters prior to the actual current density versus potential (versus reference potential) measurements, a reference nickel/nickel oxide (Ni/NiO) electrode system was fabricated. The Ni/NiO/PTFE electrode was placed in a beaker consisting of 20 wt.% KOH solution. KOH as the electrolyte and 20 wt.% as the electrolyte concentration were selected because KOH at this concentration is being used extensively in the battery, fuel cell, and water electrolysis applications. In addition, KOH also has better electrical conductivity than NaOH. Two commercial 90-10 Cu-Ni strips were used as the other electrodes of the electrochemical cell. The electrodes were connected to a computer controlled potentistatic analyzer. The analyzer system consists of a Princeton Applied Research (PAR) PARC Model 273 potentiostat, and an EG&G 5206 Lock-in Amplifier with a conventional PC, utilizing the PARC M 388 Software for system control and data accumulation.

X-RAY DIFFRACTION PARAMETERS

A Sintag XDS-2000 x-ray diffractometer with a CuKα1 source at 8048 eV, - 2.5 FWHM was used during this investigation.

The x-ray energy, current and the foil thickness (for the x-rays to penetrate through the test foil surface that is exposed to the test solution prior to the x-ray reflection to the detector system) were 35 KV, 30 mA and 12.5 μm (0.0005") respectively.

TEST PROCEDURE

The test cell was filled with the 25 wt.% KOH solution that was pre-electrolyzed in order to remove any cationic impurities. Due care was taken during the filling of the test cell to ensure that no air bubbles were trapped between the copper - nickel foil and the solution. The test cell was attached to the x-ray unit and the electrochemical testing was

initiated. Four pre-selected constant potentials (- 0.5 V, - 0.10 V, 0.5 V and + 0.10 V) were applied continuously during each electrochemical study period of nearly 48 hours.

In order to follow the structural changes during the electrochemical process, x-ray diffraction patterns were obtained after 1, 1.5, 2, 3, 4, 6 and 24 hours. Each x-ray diffraction run took 20 minutes. For convenience, we have labeled the x-ray diffraction patterns as those obtained after 1, 1.5, 2, 4, 6 and 24 hours only.

x-RAY PHOTOELECTRON SPECTROSCOPY (XPS)

X-ray photoelectron spectroscopy (XPS) was used to examine the nature of the surface reactions that were the subject of this research effort. It was also used to study the nature of the initial oxides formed on the test foils. XPS involves exposing the surface of

interest to x-rays of a discrete energy. In the Kratos model XSAM 800 surface analyzer used in these experiments, AlKα (1486.6 eV, - 0.85 FWHM) was the radiation source. This radiation interacts with the specimen, causing the material to emit electrons whose-energy is characteristic of the atoms from which they were emitted. The XPS equipment has an electron energy analyzer, which measures the kinetic energy of the emitted electrons. This measurement is made with a hemispherical analyzer having an aberration-compensated input lens (ACIL). The analyzer superimposes different voltages on the inner and outer hemispheres, which then allow only electrons with energies between these two values to pass through to the detector at the opposite end of the analyzer. The equipment scans the voltages on the two hemispheres through an energy range in steps, and during its dwell time at each step it keeps track of the counts per second, or intensity of electrons. This information can then be graphed as electron energy versus intensity. The major limit on the energy-resolving capabilities of the instrument is the width of the exciting radiation, e.g. 1.0 eV at full-width half maximum for Al Kα.

The XPS spectrometer and specimen are contained within an ultra-high vacuum. This prevents the electrons from being scattered by gas molecules before they reach the analyzer and allows experiments to be conducted and data acquired in reasonable times before the specimen surfaces are contaminated with unwanted gases and carbon from the atmosphere. This latter point is important since the XPS method analyzes for elements on the surface and within only several atomic layers of the surface. The surface sensitivity of the XPS method arises from its ability to measure the energy of emitted electrons. These electrons have a very short mean free path in solid matter. Typically,

this distance is on the order of 5 to 10 angstroms. Therefore, the emitted electrons represent elements present in the outer layer or several atomic layers below the surface.

The concentration of a given element in the surface is represented by the intensity of electrons (counts per second) emitted at a given characteristic energy. The area under these peaks in the XPS spectrum is used as a measure of the intensity. Computer-aided routines are used to perform the necessary background subtraction around the peak of interest and to calculate the area under the peak. If peaks partially overlap, a peak synthesis routine is used to extract the peak of interest. All intensities are then corrected by a multiplication factor, which represents the spectrometer efficiency and the probability of emission from a particular electron energy level in a given atom. These correction factors were determined by the analyzer's manufacturer. To assist in identifying the chemical state of the metal foils after corrosion testing, XPS spectra were made of standards of pure nickel. The nickel foil may have an oxide layer that is nonconductive and charge up during the spectra acquisition. This can cause the peaks to shift from the normal location. To correct for this, the adventitious carbon peak found on these standards was referenced to the carbon peak at 284.6 eV and all other peak locations were corrected accordingly. In the case of the partially overlapping peaks, a peak synthesis routine was used to separate and identify each contribution.

The details of the analysis parameters used to acquire the XPS data are :

- Al excitation (1486.6 eV)
- Fixed analyzer transmission
- True time averaging
- Low magnification
- Start energy of scan, 1200 eV
- Step size, 0.5 eV

- Low resolution • Channels, 2400 • Dwell, 0.5 s.

The experimental procedure adopted for obtaining the XPS spectrum and for the spectral analysis is as follows: First, a sample surface analysis survey scan in the binding energy range 0 – 1200 eV was made in order to ensure that all the relevant elements are identifiable. A series of regional scans for required elements (viz. Cu, Ni, O and C) was made. The range of the scan was within $\pm$ 10 eV of the corresponding binding energy. In order to minimize any chemical changes that may result due to surface heating, prior to the acquisition of the XPS spectra, no sputter cleaning of the surface was made. This is because sputter cleaning may induce some chemical changes (viz. Oxidation) due to local heating

In order to obtain the maximum information for all elements at a minimum time, only one energy sweep per element was made. Once the XPS spectra was obtained, a peak synthesis routine was used to match real data peaks / curves of interest.

INTERFACE STRUCTURE IDENTIFICATION PROCEDURE

For the foil thickness used in this investigation, it is reasonable to suggest that the x-ray diffraction patterns represent the cumulative structure of metal and the metal/liquid interface. Since, the interface region is composed of both the inner passive layer and the outer passive layer, it is reasonable to assign the x-ray diffraction data to represent the structure of the base metal and the inner and outer passive layers.

The information acquired in the XPS data represents the structure of the top few layers of the electrochemically reacted surface. Since the top few layers are contained in the outer passive layer (Figure 1), the XPS analysis can be suggested to provide information on the outer passive layer without being obscured with the information from the inner passive layer or the bulk material. By subtracting the structure of the outer passive layer (obtained from XPS data) from the XRD structural information, the inner passive layer structure can be established.

RESULTS

Figure 3 shows a typical x-ray diffraction pattern obtained from a 12.5 μm (0.0005") thick 90-10 Cu-Ni foil mounted on the test cell. The results suggest that the test sample surfaces are not significantly oxidized.

Figure 4 shows a typical current versus applied potential plot of the 90-10 Cu-Ni foil in KOH solution as it cycles once through from - 1.0 V → + 1.0 V→ - 1.0 V. The results (shown in Figure 4) suggest that as the transition between a cathodic and anodic chemical reaction occurs over a very narrow potential range (- 10 mV - + 10 mV). The current remains independent of potential over the potential range investigated (i.e. 10 to 1000 mV and/or –10 to – 1000 mV).

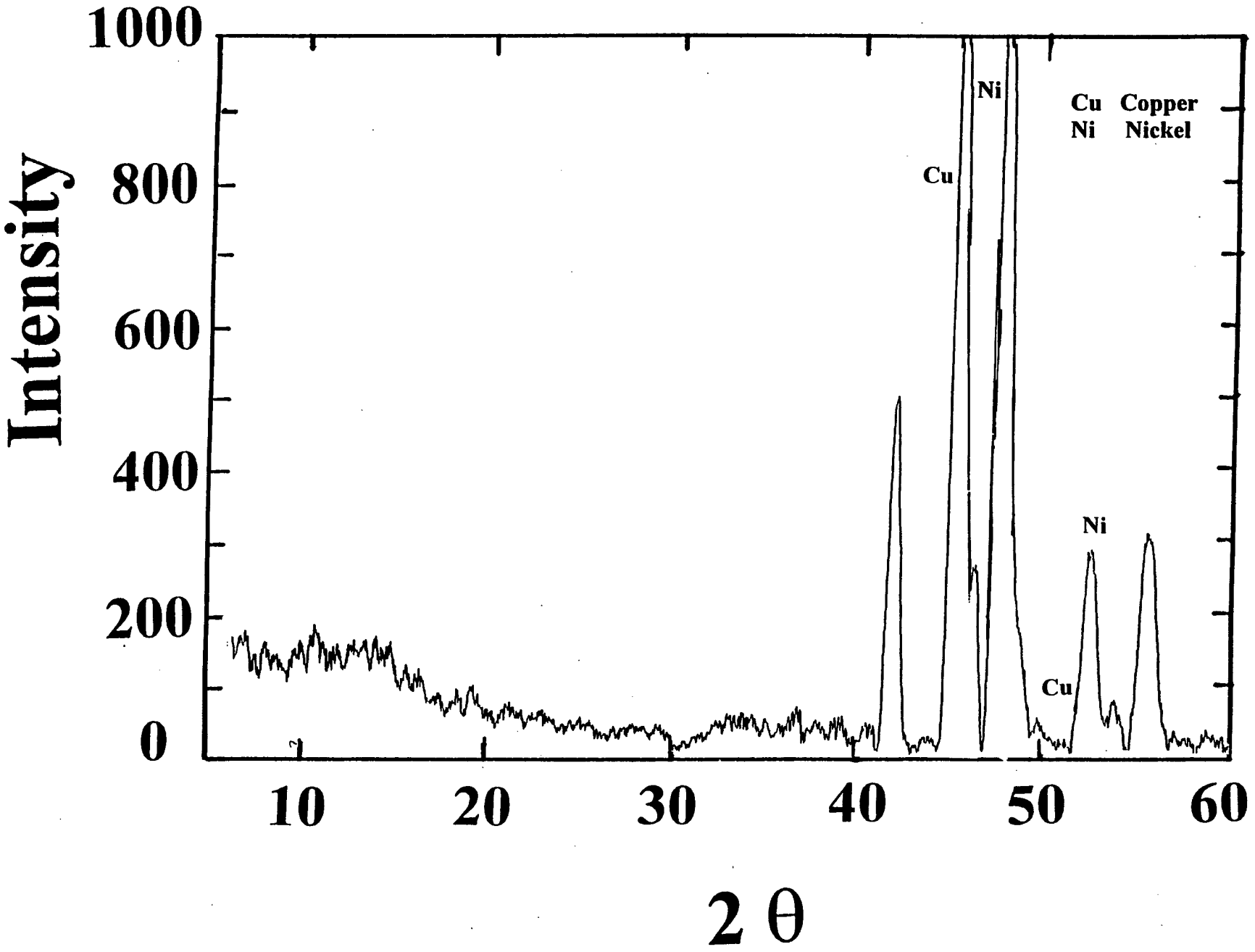

Figure 3. Typical x-ray diffraction pattern obtained from 90 % copper 10 % nickel foil mounted on the electrochemical test cell.

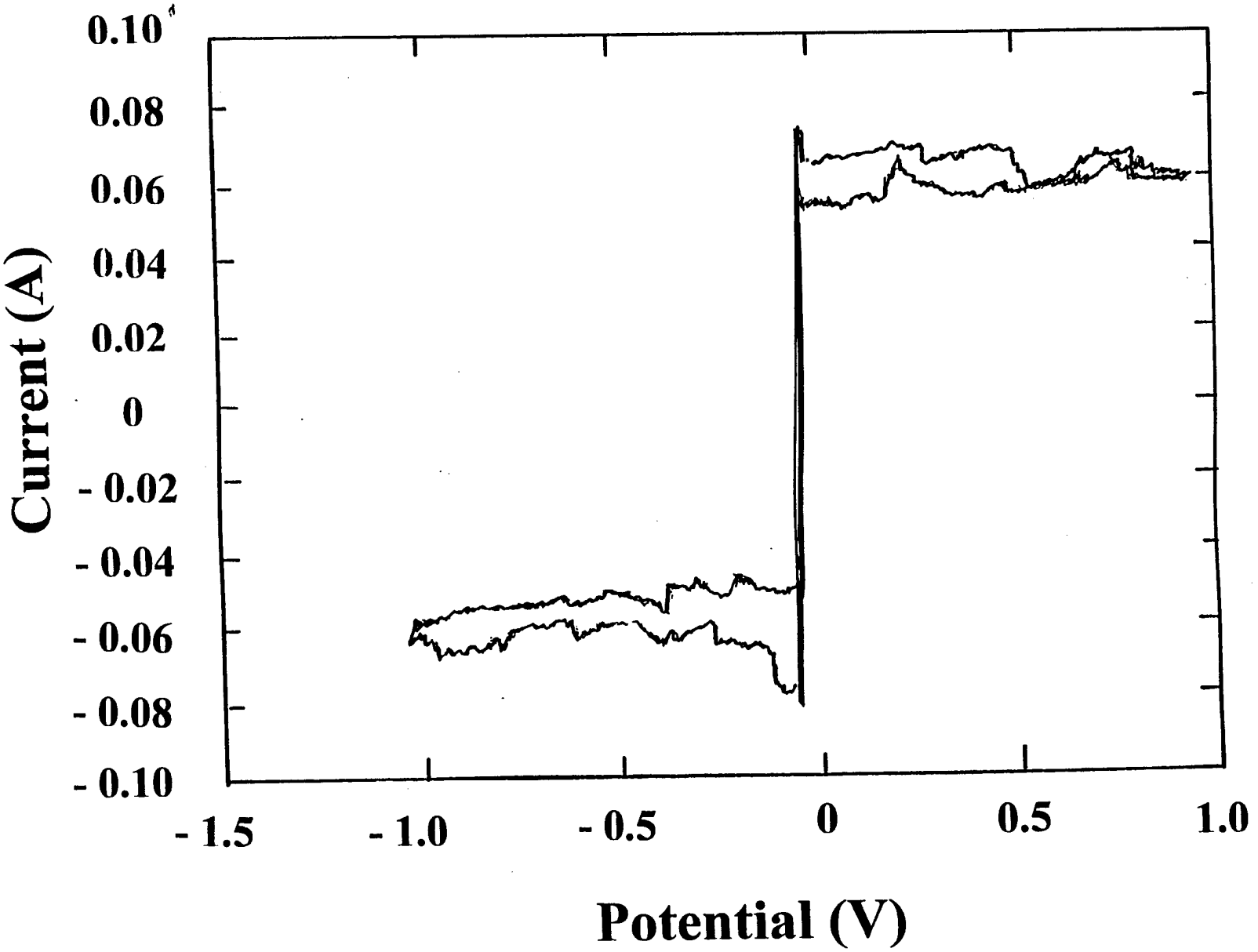

Figure 4. Current versus applied potential (versus reference potential) plot of 90 % copper – 10 % nickel/KOH system at room temperature.

XRD RESULTS FOR POTENTIALS OF – 500 mV and – 100 mV

It was found that when a cathodic potential of either – 0.5 V or - 0.10 V was applied, during the first 60 minutes, no significant changes were observed in the diffraction pattern. However, a careful examination of x-ray scans acquired later revealed that the possible changes were masked by the system's background noise. After two hours, significantly measurable differences in the diffraction patterns were observed. Figures 5 - 8 show x-ray diffraction patterns obtained after 2, 4, 6 and ~ 24 hours of exposure to a constant potential of – 0.5 V. Between 24 - 48 hours, the test samples tended to develop fine pores and the electrolyte would seep through the exposed film surface. Some foils were completely destroyed due to contact with the KOH solution over long periods of time leaving blackish colored fragments of the alloy. Samples that were not completely dissolved by the electrolyte showed copper color. The clear electrolyte solution developed a deep blue color after approximately 2 hours. The diffraction patterns were analyzed. It was found that the peaks for NIOOH and $Ni(OH)_2$ underwent appreciable increases. Figures 9 - 10 show x-ray diffraction patterns obtained after 4 and ~ 24 hours of exposure to a constant potential of – 0.1 V. Between 24 - 48 hours, the test samples tended to develop fine pores and the electrolyte would seep through the exposed film surface. From the above x ray diffraction results, the progression of chemical reaction can be suggested as follows:

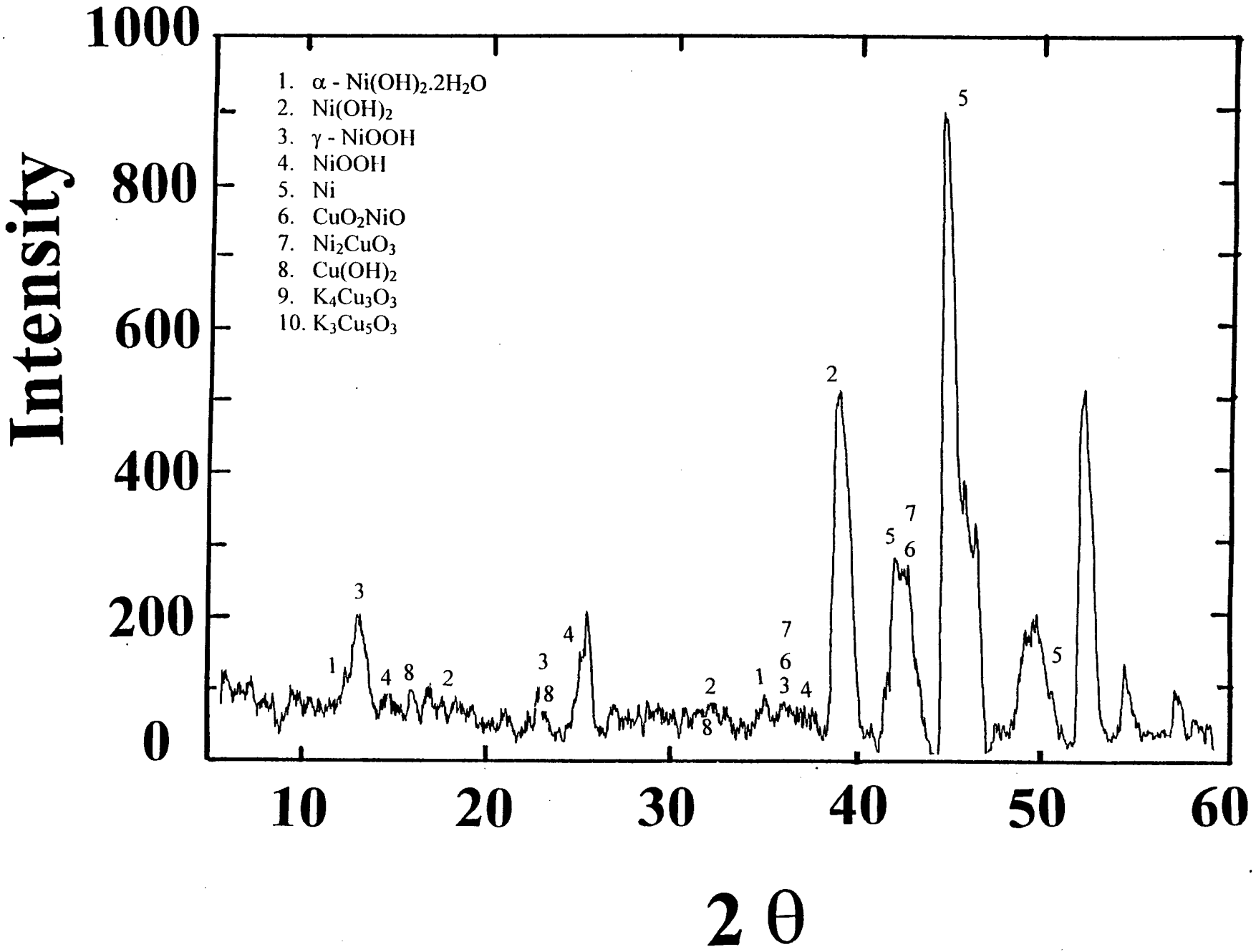

Figure 5. In-situ x-ray diffraction pattern obtained for 12.5 μm (0.0005") thick 90 – 10 Cu – Ni foil mounted on the electrochemical test cell, after exposure for 2 hours at - 0.50 V versus a Ni/NiO electrode.

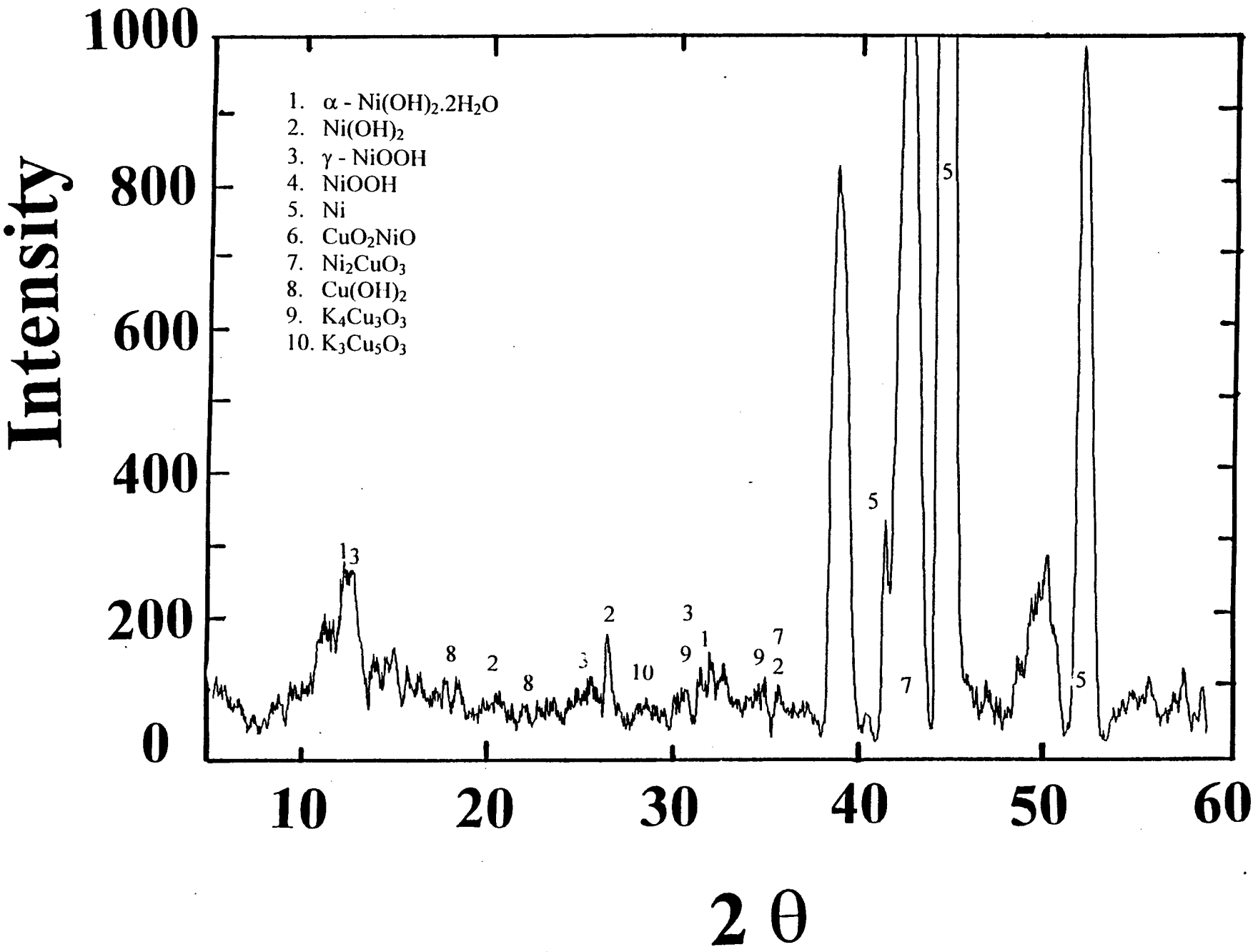

Figure 6 In-situ x-ray diffraction pattern obtained for 12.5 μm (0.0005") thick 90 – 10 Cu – Ni foil mounted on the electrochemical test cell, after exposure for 4 hours at - 0.50 V versus a Ni/NiO electrode.

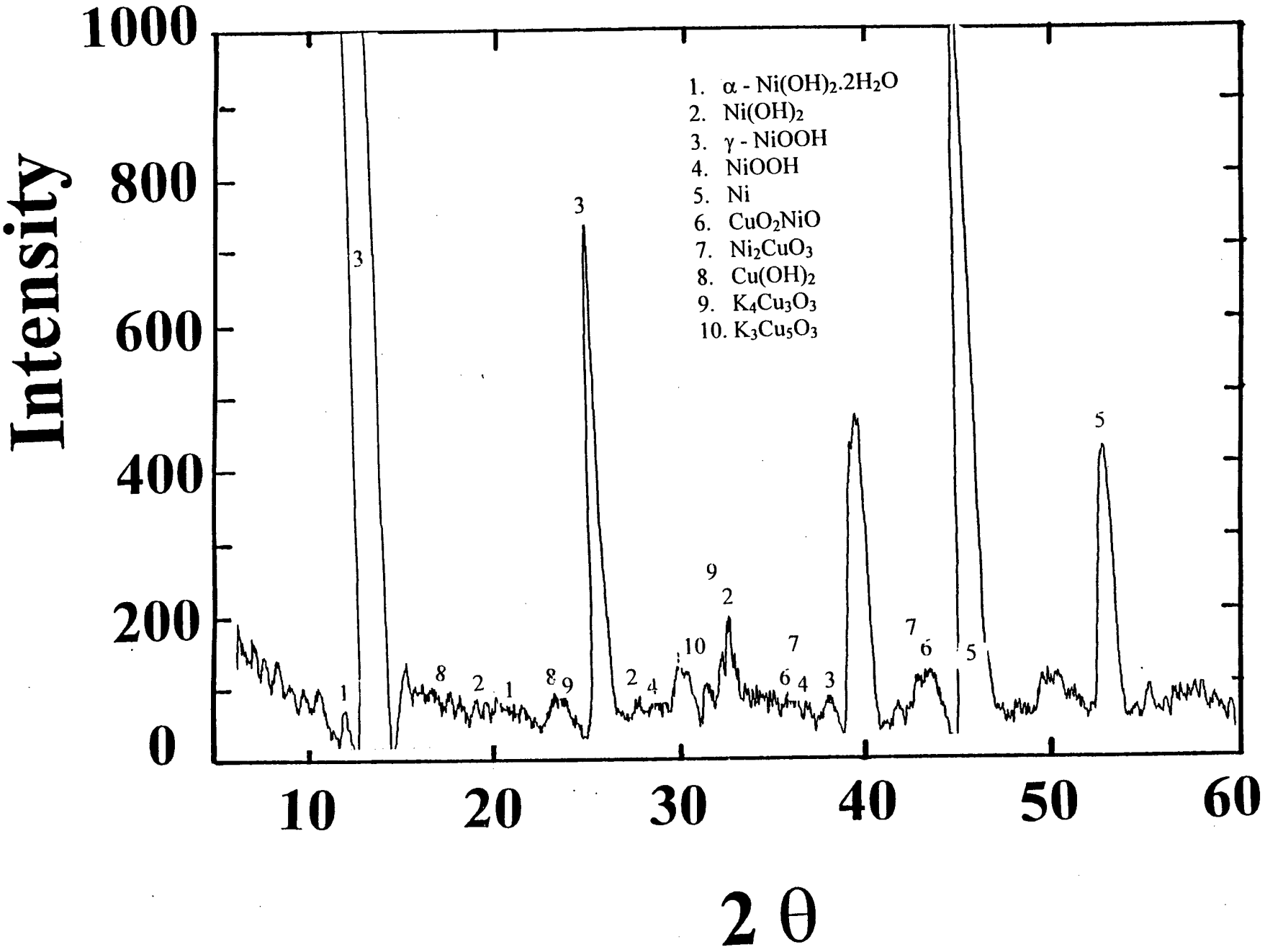

Figure 7. In-situ x-ray diffraction pattern obtained for 12.5 μm (0.0005") thick 90 – 10 Cu – Ni foil mounted on the electrochemical test cell, after exposure for 6 hours at - 0.50 V versus a Ni/NiO electrode.

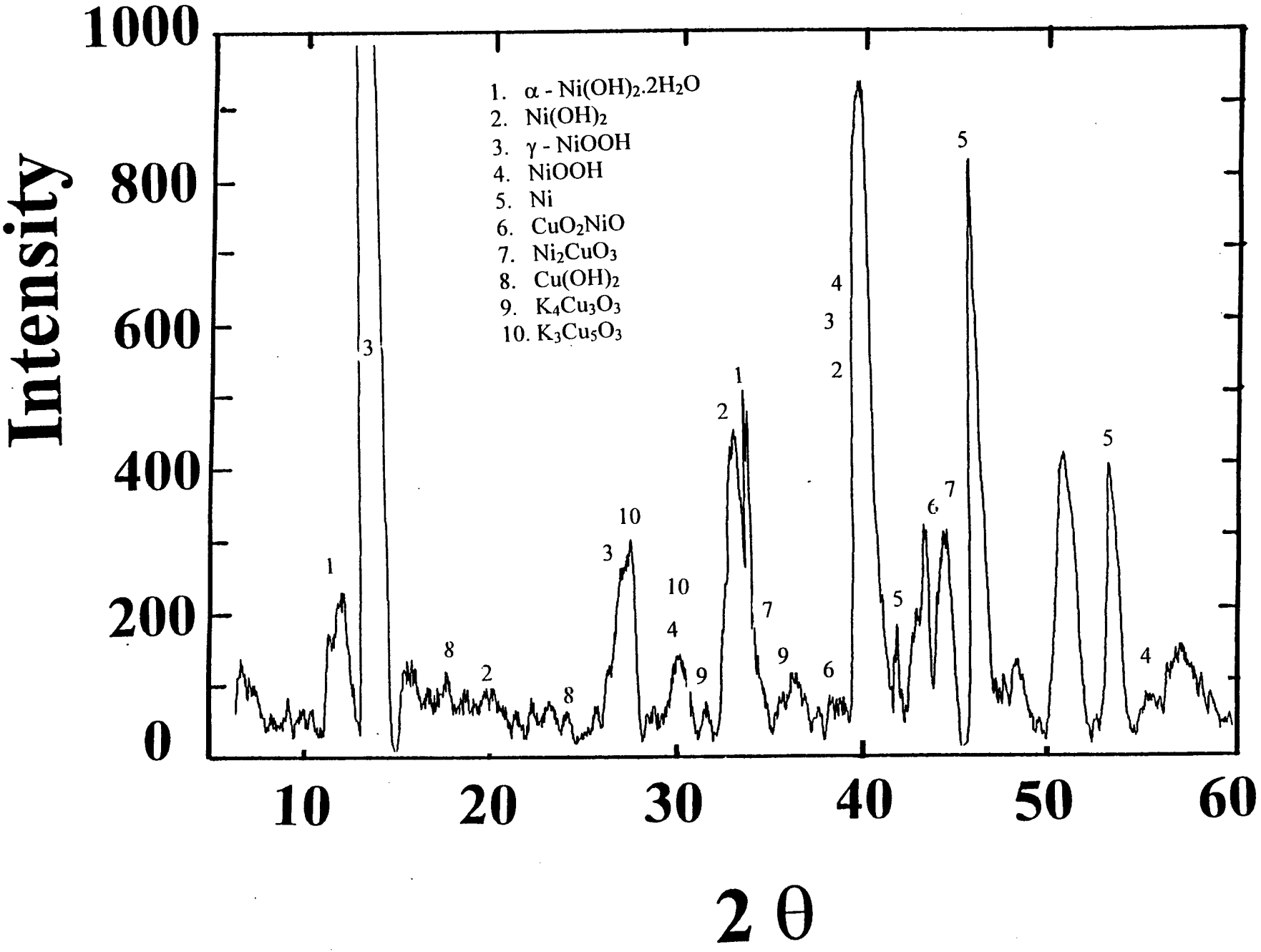

Figure 8. In-situ x-ray diffraction pattern obtained for 12.5 μm (0.0005") thick 90 – 10 Cu – Ni foil mounted on the electrochemical test cell, after exposure for 24 hours at - 0.50 V versus a Ni/NiO electrode.

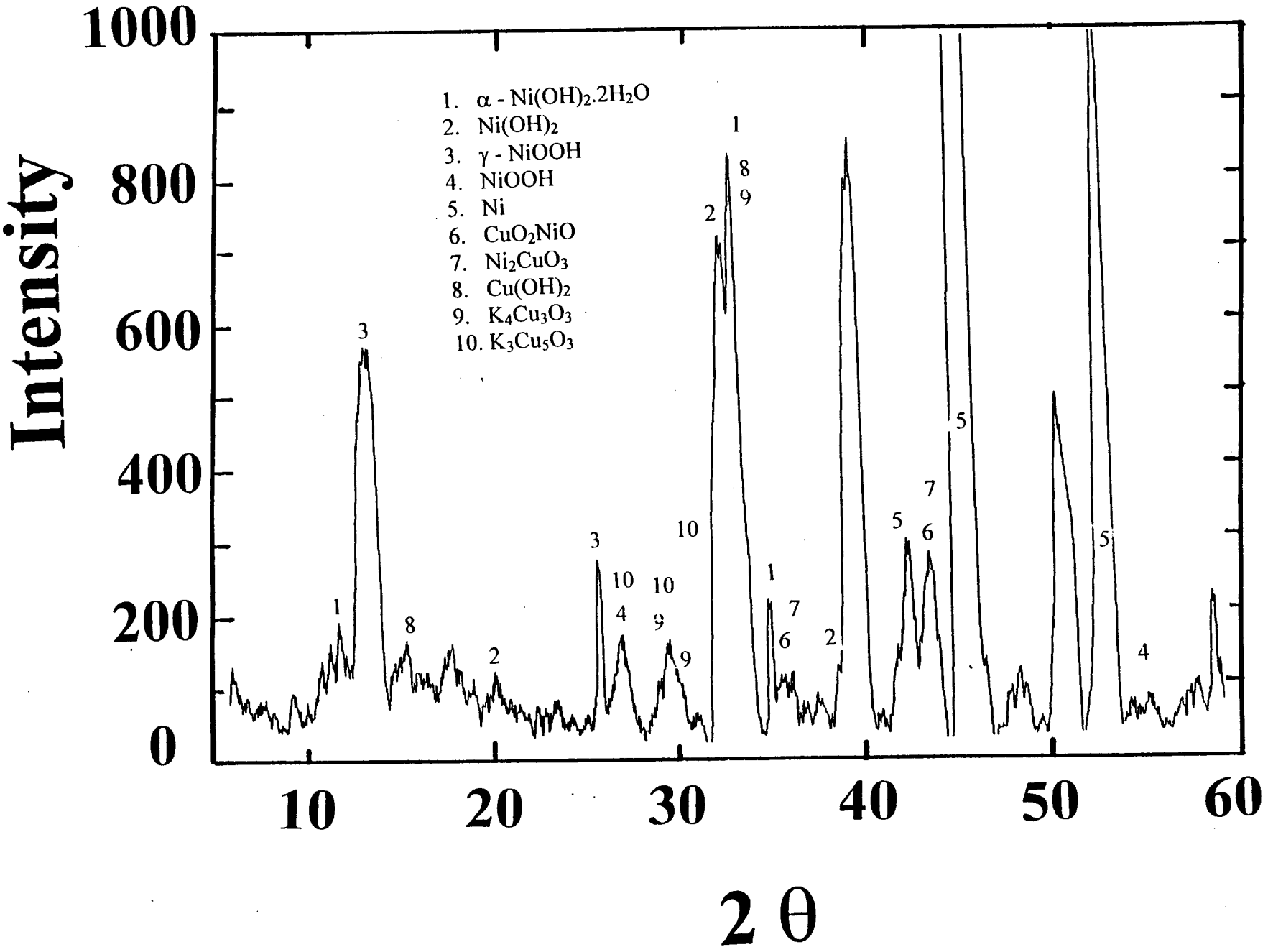

Figure 9. In-situ x-ray diffraction pattern obtained for 12.5 μm (0.0005") thick 90 – 10 Cu – Ni foil mounted on the electrochemical test cell, after exposure for 4 hours at - 0.10 V versus a Ni/NiO electrode.

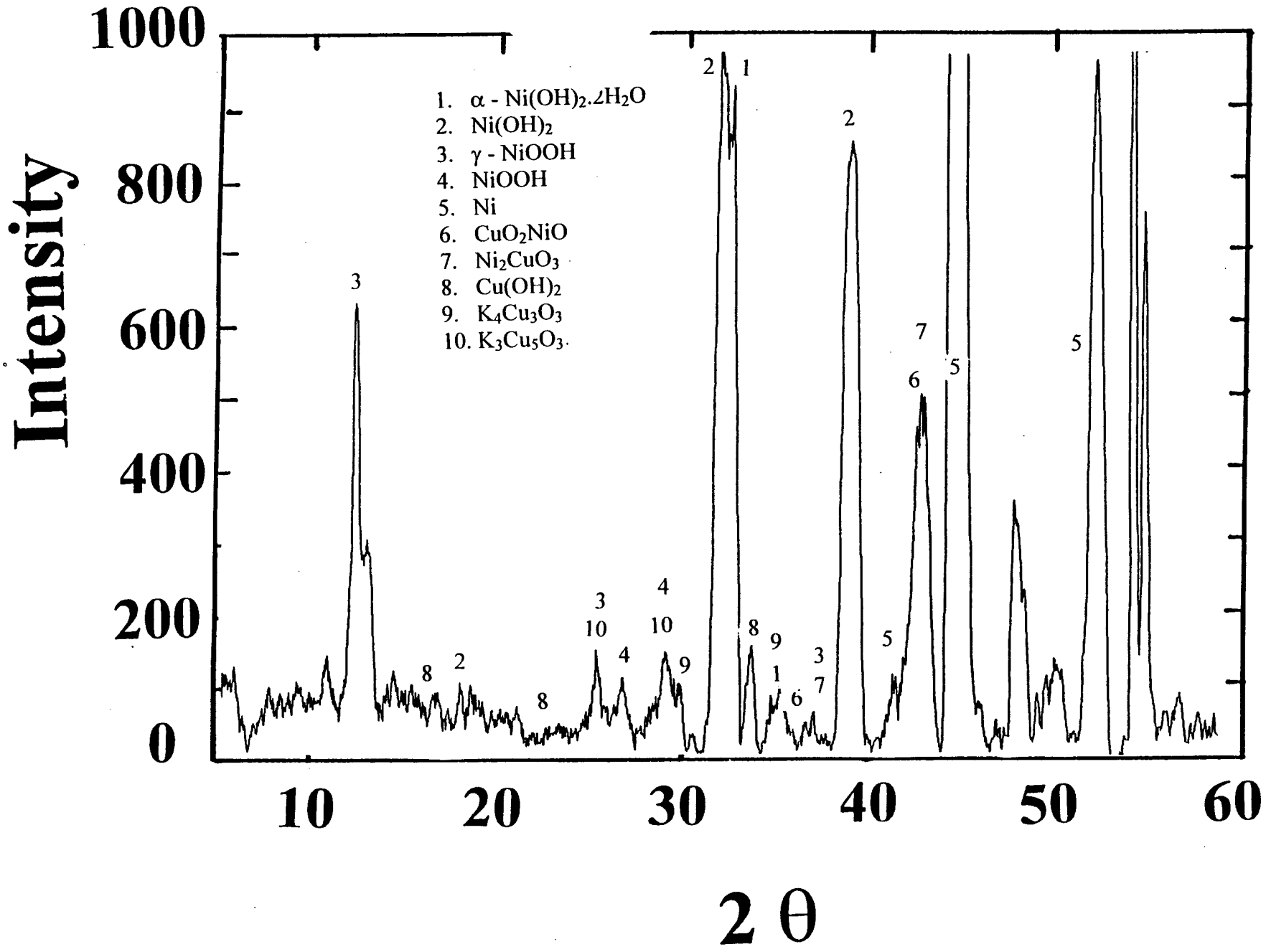

Figure 10. In-situ x-ray diffraction pattern obtained for 12.5 μm (0.0005") thick 90 – 10 Cu – Ni foil mounted on the electrochemical test cell, after exposure for 24 hours at - 0.10 V versus a Ni/NiO electrode.

When a constant negative potential (- 0.5 or – 0.1 V) was continuously applied, the cathodic reaction progresses with the accumulation of OH at the cathode and the reaction at the alloy / KOH interface can be represented as follows:

$Ni^{+3} \Rightarrow Ni(OH)_2 \Rightarrow H_2 \uparrow$ $\quad$ $Cu^{+2} \Rightarrow Cu(OH)_2 \Rightarrow H_2 \uparrow$

$H_2O \Rightarrow OH^- + \frac{1}{2} H_2 \uparrow$

The x-ray diffraction results obtained during the present investigation indicate that at this negative potential (-0.5 V and – 0.1 V), in addition to the presence of $Ni(OH)_2$, $Cu(OH)_2$ and $Cu_2O.NiO$, there is a significant formation of NiOOH and CuO. Although the formation of $Ni(OH)_2$, $Cu(OH)_2$ are expected during electrochemical reaction at – 0.5 and – 0.1 V, the observed presence of NiOOH, $Cu_2O.NiO$ and CuO would not be expected.

The presence of NiOOH and CuO can be explained only if one assumes that immediately after the introduction of KOH into the electrochemical cell, the top layers of the 90-10 Cu-Ni that are in contact with the KOH underwent oxidation and formed NiOOH and CuO. As soon as the negative potential was applied, the cathodic reaction begins. As a result the NiOOH and CuO were reduced to form $Ni(OH)_2$ and $Cu(OH)_2$. Thus the reaction for nickel is as follows:

$Ni^{+3} \Rightarrow Ni^{+2}(OH)_2 \Rightarrow H_2O \Rightarrow \frac{1}{2} H_2$ gas $\uparrow + (OH)^-$

$Ni^{+2}O \Rightarrow Ni^{+2}(OH)_2 \Rightarrow H_2O \Rightarrow \frac{1}{2} H_2$ gas $\uparrow + (OH)^-$

$Ni^{+3}OOH \Rightarrow Ni^{+2}(OH)_2 \Rightarrow H_2O \Rightarrow \frac{1}{2} H_2$ gas $\uparrow + (OH)^-$

Similarly, the reaction for copper can be suggested as:

$Cu^{+2} \Rightarrow Cu(OH)_2 \Rightarrow H_2O \Rightarrow \frac{1}{2} H_2$ gas $\uparrow + (OH)^-$

$Cu_2O \Rightarrow Cu(OH)_2$

$CuO \Rightarrow Cu^{+2}(OH)_2 \Rightarrow H_2O \Rightarrow \frac{1}{2} H_2$ gas $\uparrow + (OH)^-$

$Cu^{+1}{}_2O + NiO \Rightarrow Cu_2O.NiO$

XPS RESULTS FOR POTENTIALS OF – 500 mV

After the in-situ examination of the 90-10 Cu-Ni sample in KOH for 24 hours was completed, the copper - nickel foil was removed from the test cell and was rinsed with distilled water. The sample was then introduced into the sample chamber of the XPS unit and was analyzed. The total duration of sample removal from test cell, cleaning, introduction in the XPS unit, and data collection was approximately 20 minutes. Figures 11, 12 and 13 show typical XPS spectra for copper, nickel and oxygen obtained from the test foil that had been subjected to - 0.5 V in KOH solution. The peak locations for the various identified compounds were obtained from the hand book of x-ray photoelectron spectroscopy [14]..

The results in Figures 11 and 12 suggest that $Cu(OH)_2$, CuO and $Ni(OH)_2$ are present in the outer passive layer. The detected structure in Figure 13 of oxygen at 528.5 and 531.5 eV corresponds to the oxygen associated with $Ni(OH)_2$.

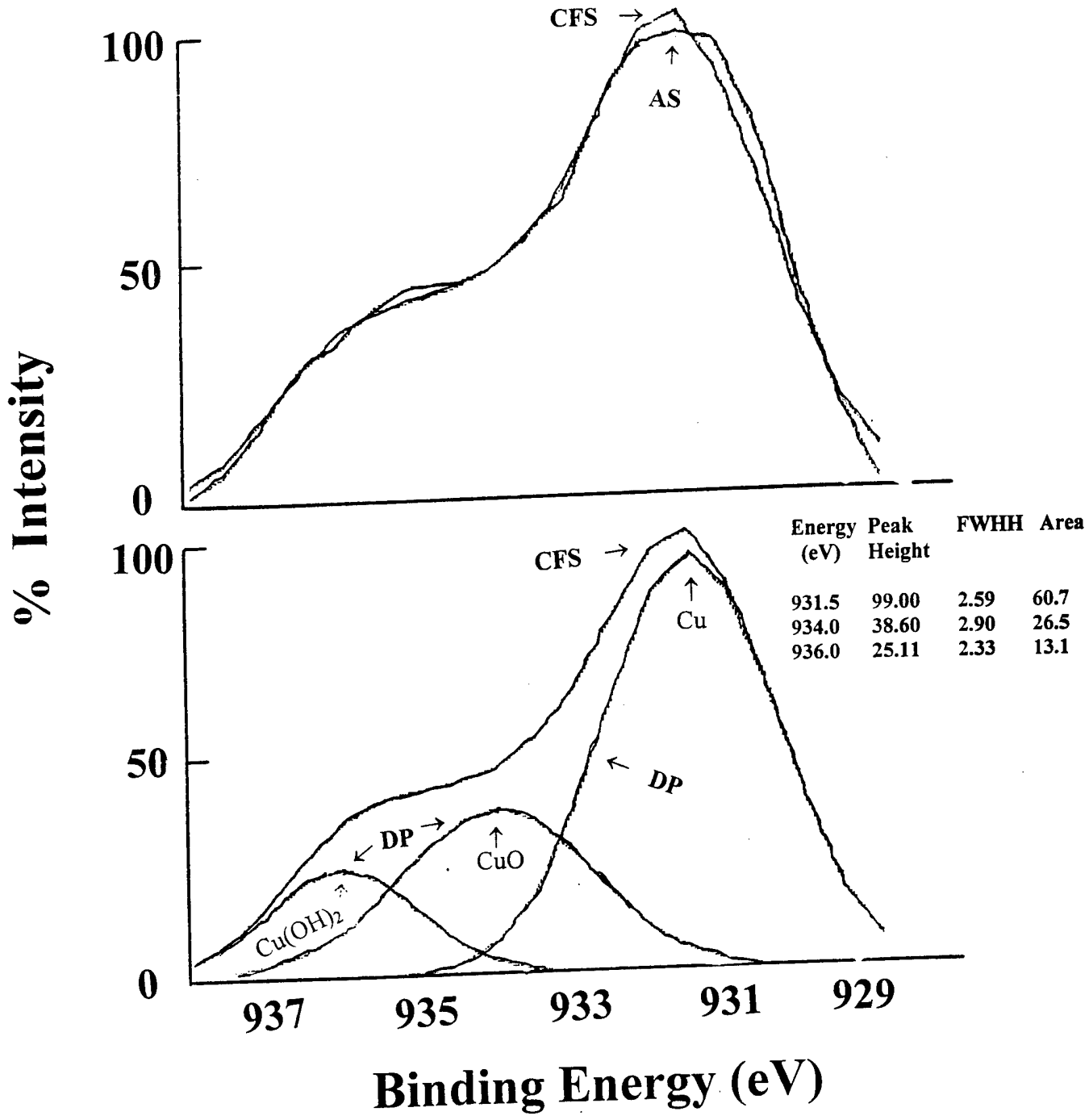

AS → **Actual XPS spectra**
CFS → **Copy of the XPS spectra generated by curve fitting**
DP → **De convoluted peaks of the curve fitted XPS spectra**
FWHH → **Full width half height**

Figure 11. Copper peaks obtained from XPS analysis of 12.5 μm (0.0005") thick 90-10 Cu-Ni foil surface exposed to the KOH at - 0.5 V for 24 hours.

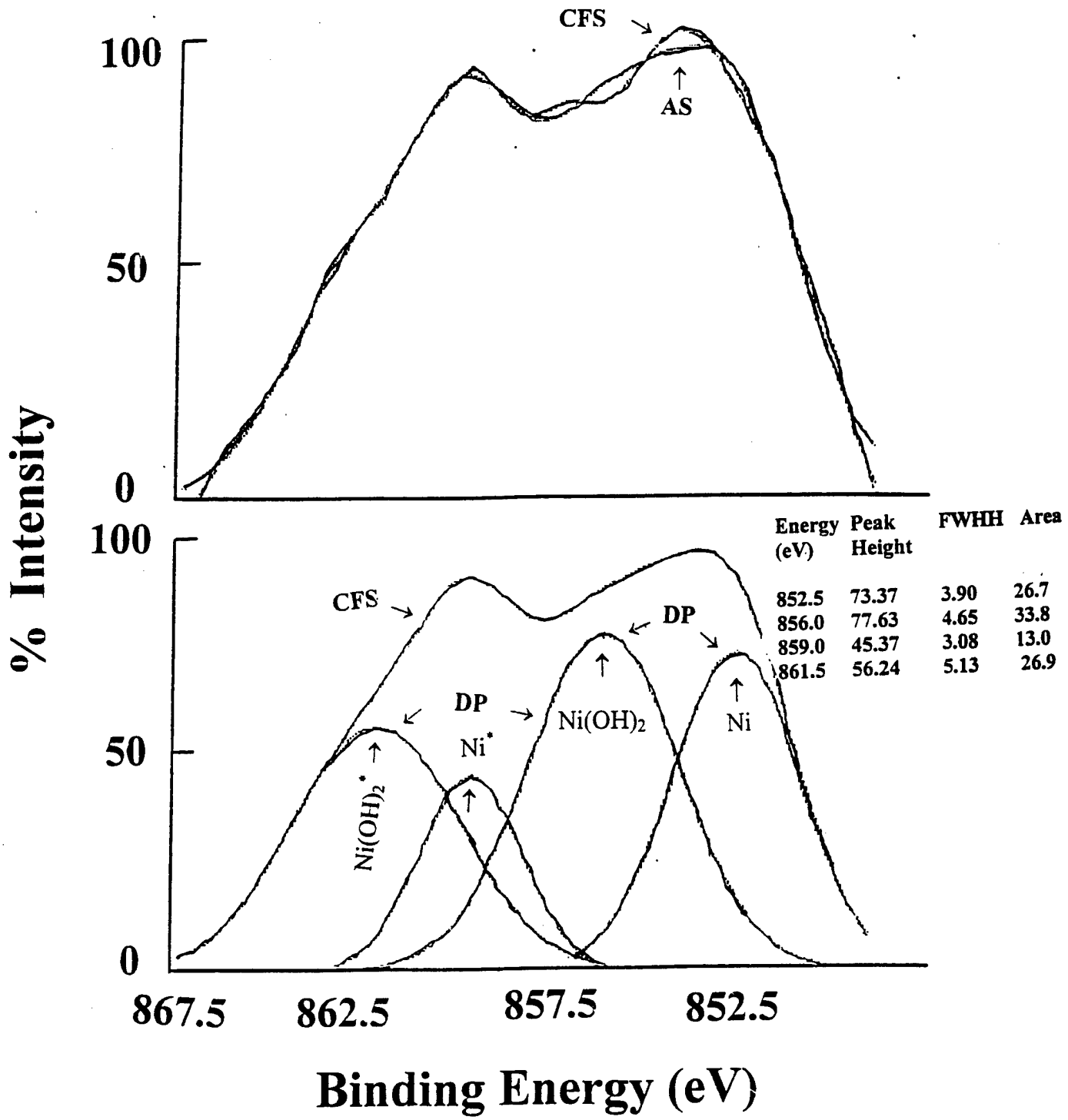

AS → **Actual XPS spectra**
CFS → **Copy of the XPS spectra generated by curve fitting**
DP → **De convoluted peaks of the curve fitted XPS spectra**
FWHH → **Full width half height**
***** → **Satellite or Minor Peak**

Figure 12. Nickel peaks obtained from XPS analysis of 12.5 μm (0.0005") thick 90-10 Cu-Ni foil surface exposed to the KOH at - 0.5 V for 24 hours.

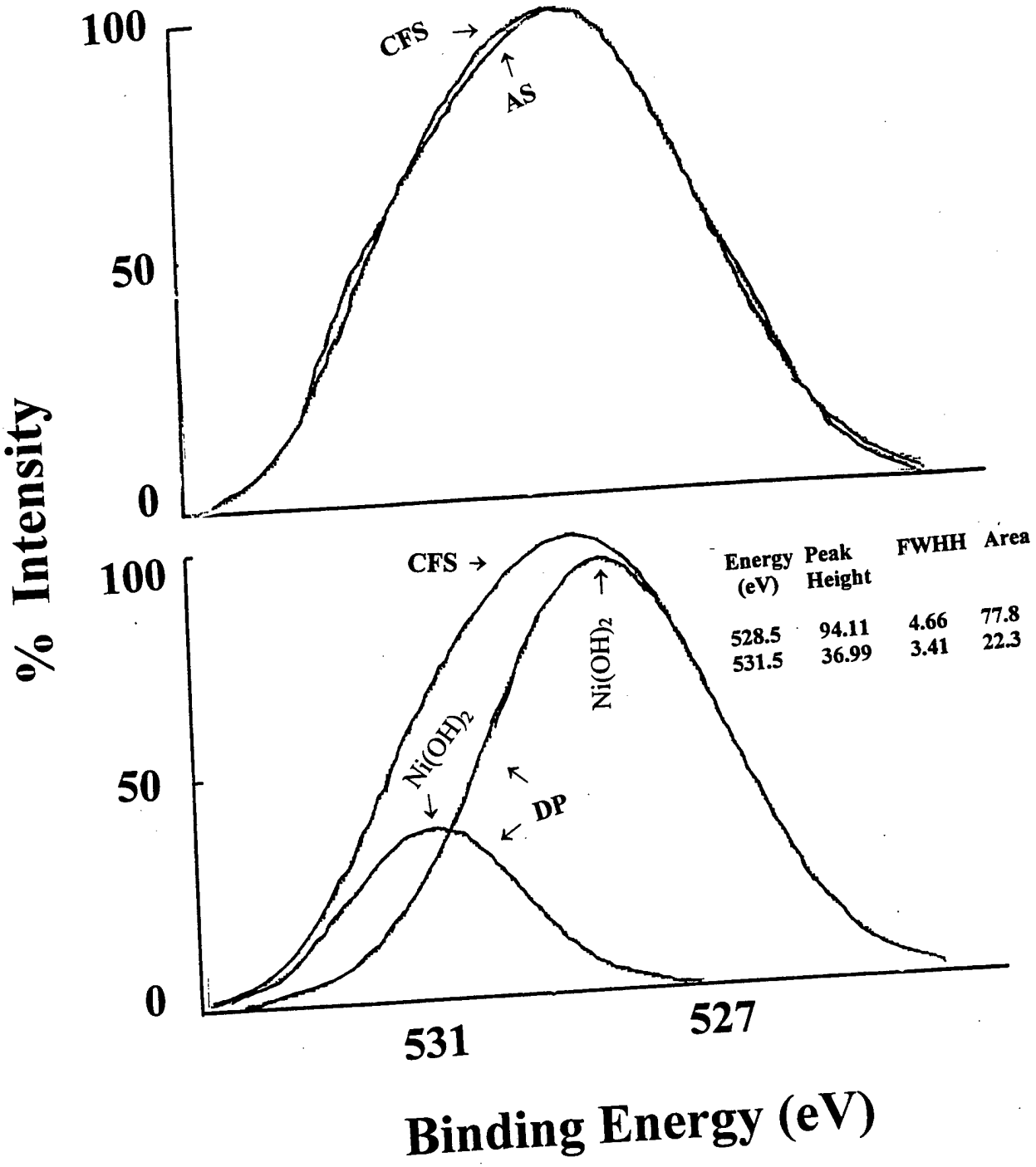

AS → **Actual XPS spectra**
CFS → **Copy of the XPS spectra generated by curve fitting**
DP → **De convoluted peaks of the curve fitted XPS spectra**
FWHH → **Full width half height**

Figure 13. Oxygen peaks obtained from XPS analysis of 12.5 μm (0.0005") thick 90-10 Cu-Ni foil surface exposed to the KOH at - 0.5 V for 24 hours.

XRD RESULTS FOR POTENTIALS OF + 500 mV and + 100 mV

The results on the 90-10 Cu-Ni foils subjected to + 0.5 V and + 0.1 V following the in-situ x-ray diffraction studies are shown in Figures 14 – 19 and 20 – 23 respectively. The figures correspond to the measurements made at time intervals of 1 (Figure 14), 2 (Figure 15), 3 (Figure 16), 4 (Figure 17), 6 (Figure 18) and 23 (Figure19) hours exposure at + 0.5 V, and 2 (Figure 20) 4 (Figure 21), 6 (Figure 22), 24 (Figure 23) hours exposure at + 0.1 V respectively. The x-ray diffraction results indicate that the interface of 90-10 Cu-Ni / KOH consists of NiO, Ni_2O_3, Ni_2CuO_3, NiOOH, $Ni(OH)_2$ NiO, $Cu(OH)_2$ and CuO. From the above results, it can be suggested that the 90-10 Cu-Ni foil is oxidized and both Ni^{+3} and Ni^{+2} states of nickel and Cu^{+1} and Cu^{+2} states of copper are present at the interface.

Therefore, we an postulate electrochemical anodic reaction for 90-10 Cu-Ni in KOH at + 0.5 V and + 0.1 V to follow the typically expected steps:

The reaction for nickel at + 0.5 and + 0.1 V is as follows:

$$Ni \Rightarrow Ni(OH)_2 \Rightarrow Ni^{+3}OOH \Rightarrow Ni^{+3}{}_2O_3 \Rightarrow Ni^{+2}O$$

and for copper the reaction can be expressed as:

$$Cu^{+2} \Rightarrow Cu(OH)_2 \Rightarrow CuO$$

$$Cu^{+1} \Rightarrow Cu^{+2}{}_2O \Rightarrow CuO$$

$$Cu^{+1}O + Ni^{+2}O \Rightarrow Cu^{+1}{}_2.NiO$$

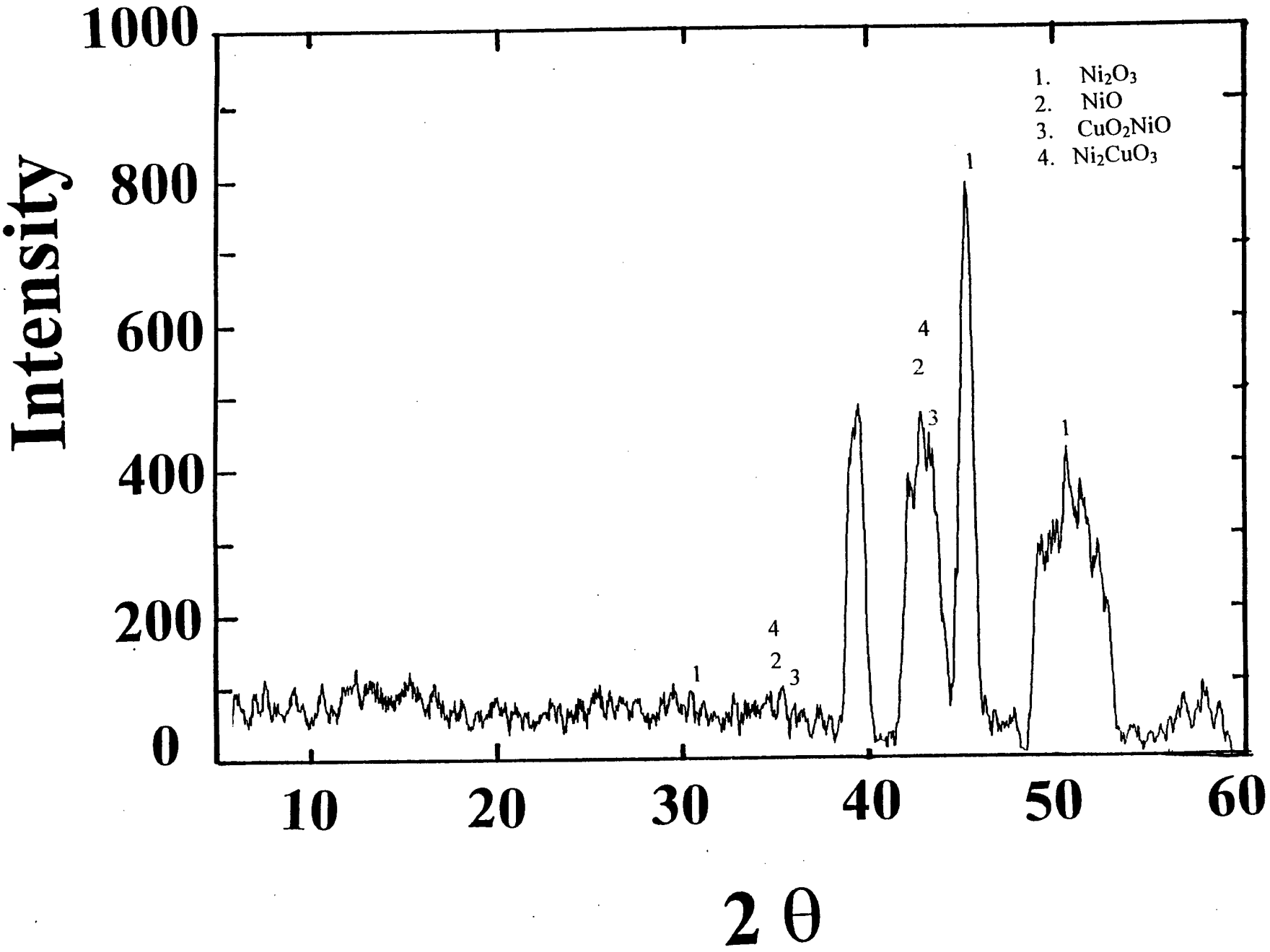

Figure 14. In-situ x-ray diffraction pattern obtained for 12.5 μm (0.0005") thick 90 – 10 Cu – Ni foil mounted on the electrochemical test cell, after exposure for 1 hour at + 0.5 V versus a Ni/NiO electrode.

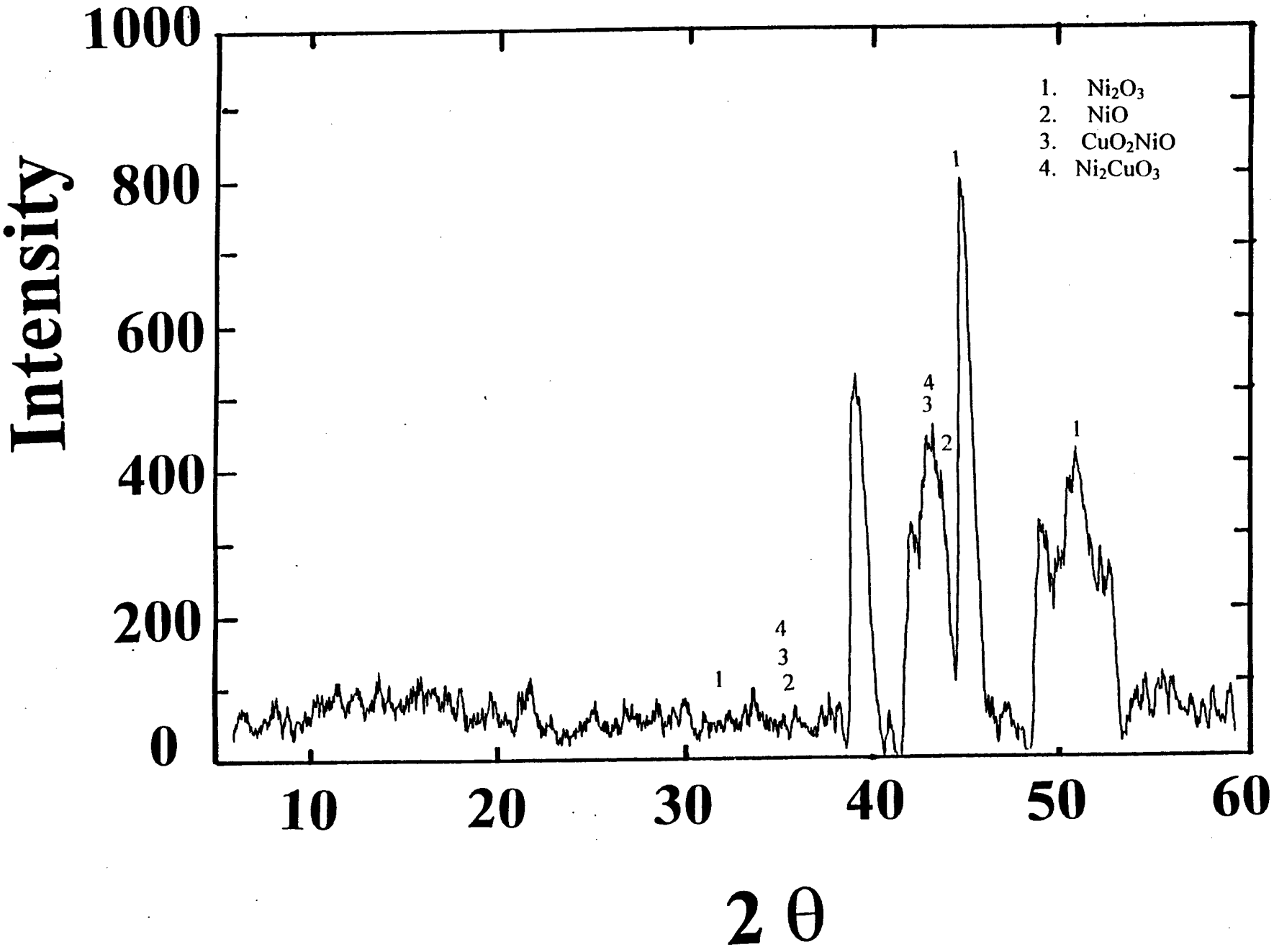

Figure 15. In-situ x-ray diffraction pattern obtained for 12.5 μm (0.0005") thick 90 – 10 Cu – Ni foil mounted on the electrochemical test cell, after exposure for 2 hours at + 0.5 V versus a Ni/NiO electrode.

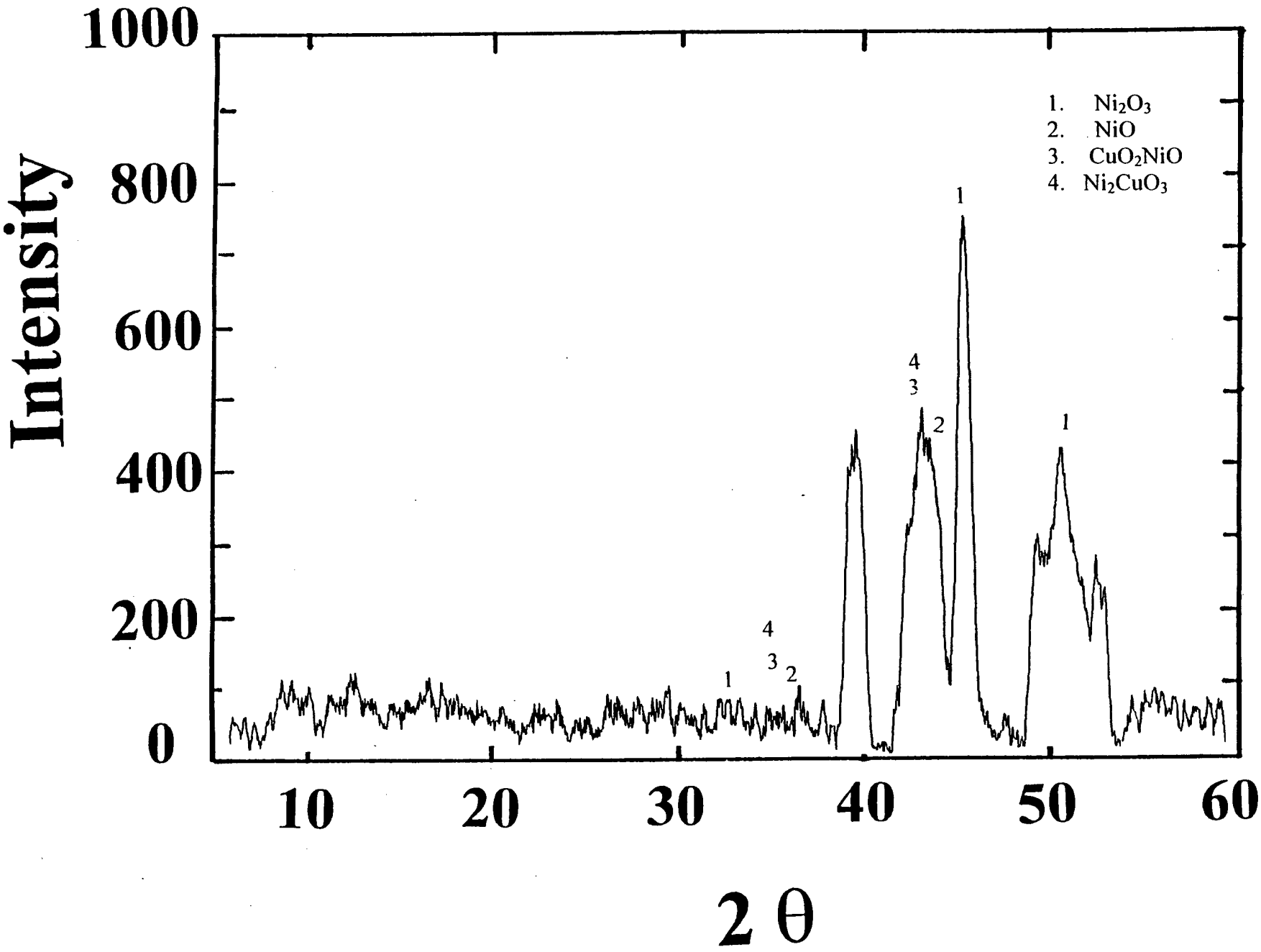

Figure 16 In-situ x-ray diffraction pattern obtained for 12.5 μm (0.0005") thick 90 – 10 Cu – Ni foil mounted on the electrochemical test cell, after exposure for 1 hours at + 0.5 V versus a Ni/NiO electrode.

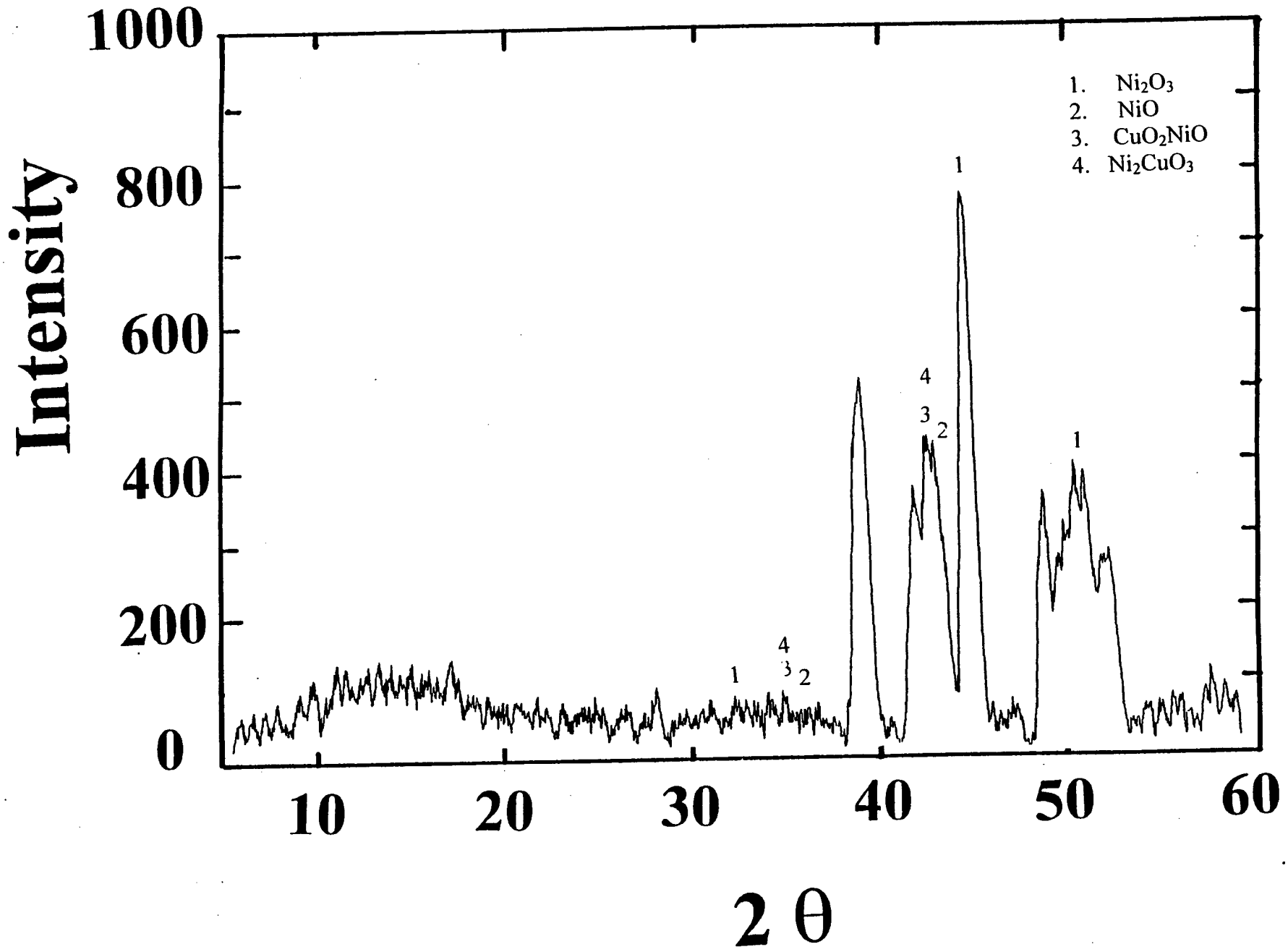

Figure 17. In-situ x-ray diffraction pattern obtained for 12.5 μm (0.0005") thick 90 – 10 Cu – Ni foil mounted on the electrochemical test cell, after exposure for 4 hours at + 0.5 V versus a Ni/NiO electrode.

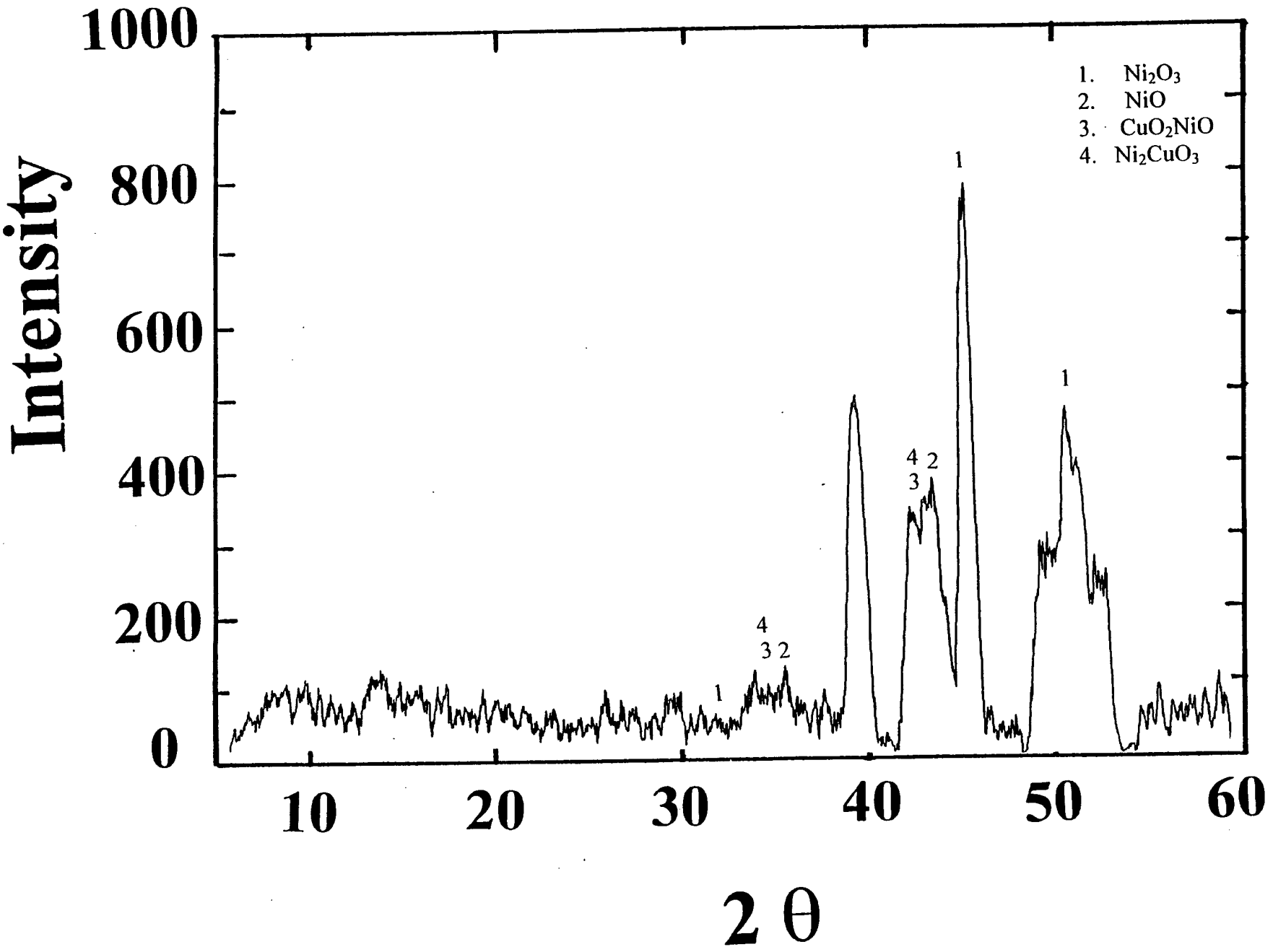

Figure 18. In-situ x-ray diffraction pattern obtained for 12.5 μm (0.0005") thick 90 – 10 Cu – Ni foil mounted on the electrochemical test cell, after exposure for 6 hours at + 0.5 V versus a Ni/NiO electrode.

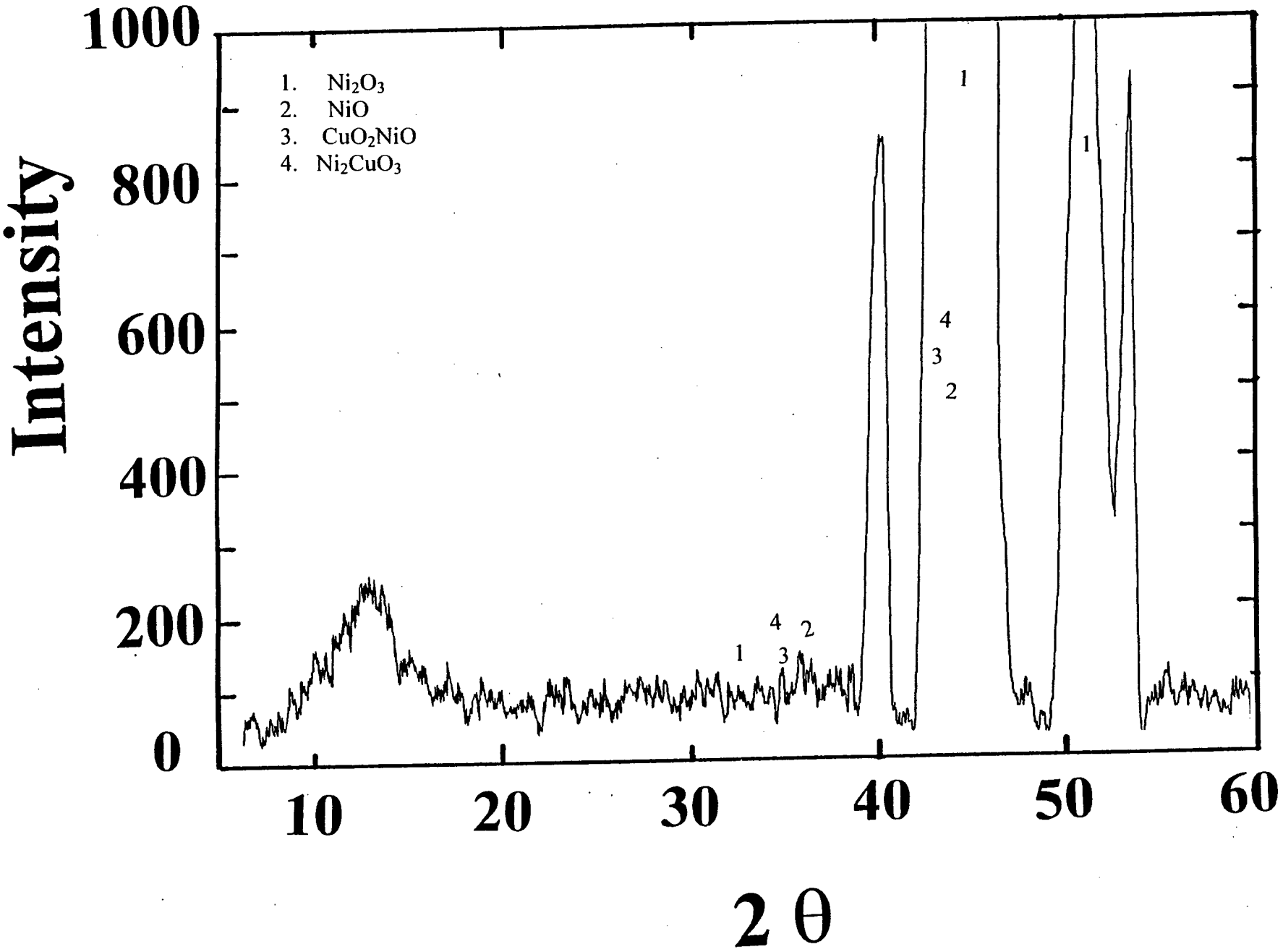

Figure 19. In-situ x-ray diffraction pattern obtained for 12.5 μm (0.0005") thick 90 – 10 Cu – Ni foil mounted on the electrochemical test cell, after exposure for 24 hours at + 0.5 V versus a Ni/NiO electrode.

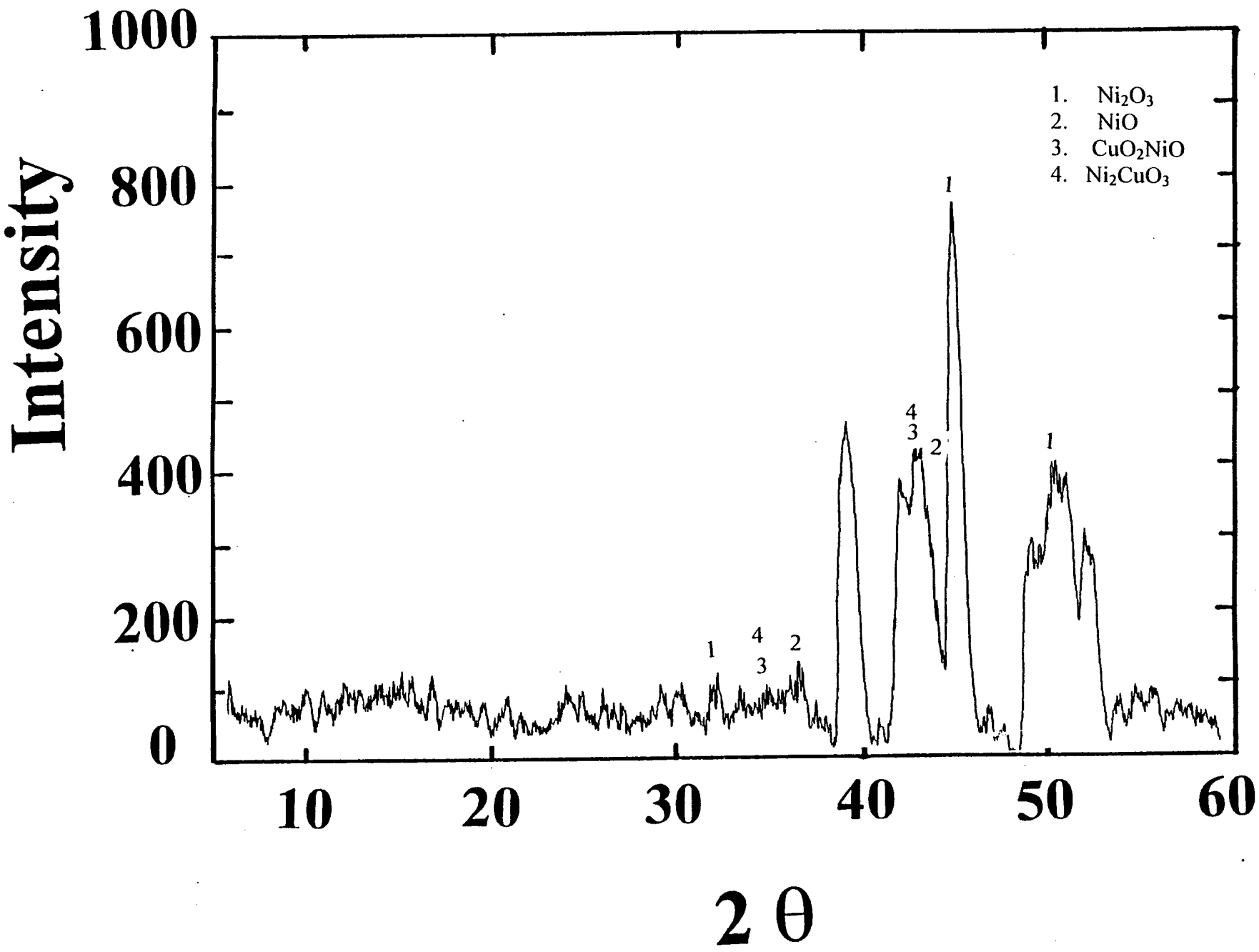

Figure 20. In-situ x-ray diffraction pattern obtained for 12.5 μm (0.0005") thick 90 – 10 Cu – Ni foil mounted on the electrochemical test cell, after exposure for 2 hours at + 0.1 V versus a Ni/NiO electrode.

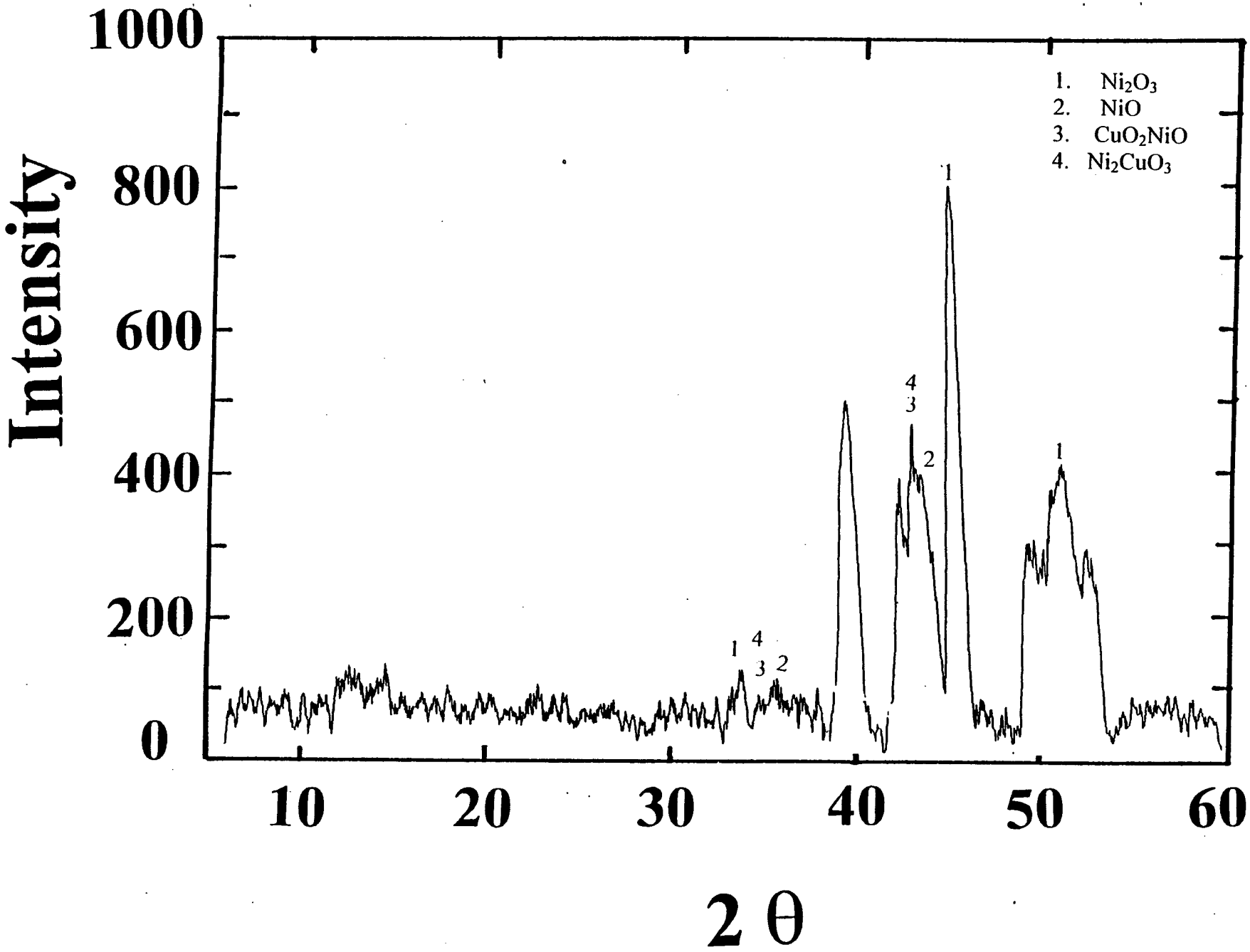

Figure 21. In-situ x-ray diffraction pattern obtained for 12.5 μm (0.0005") thick 90 – 10 Cu – Ni foil mounted on the electrochemical test cell, after exposure for 4 hours at + 0.1 V versus a Ni/NiO electrode.

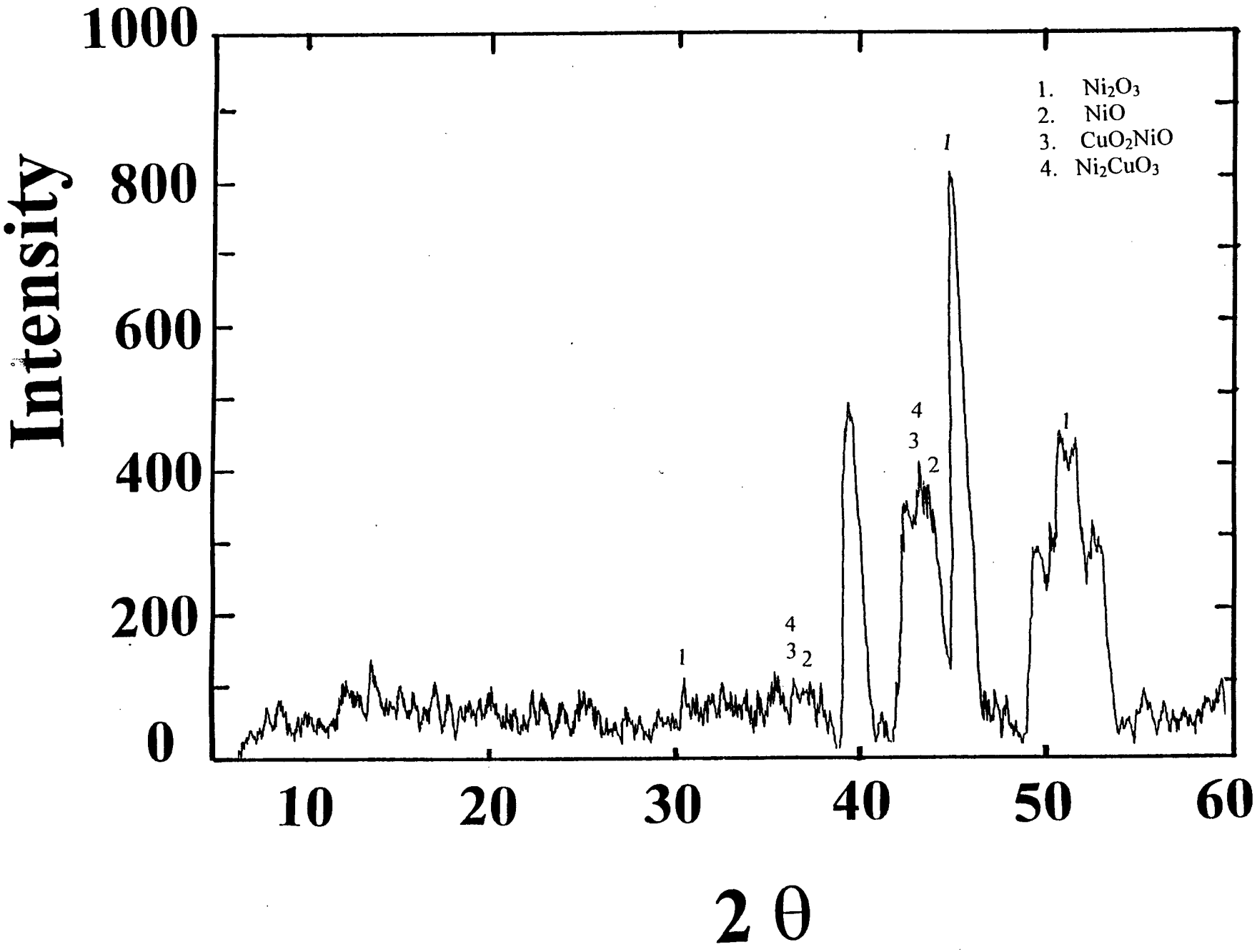

Figure 22. In-situ x-ray diffraction pattern obtained for 12.5 μm (0.0005") thick 90 – 10 Cu – Ni foil mounted on the electrochemical test cell, after exposure for 6 hours at + 0.1 V versus a Ni/NiO electrode.

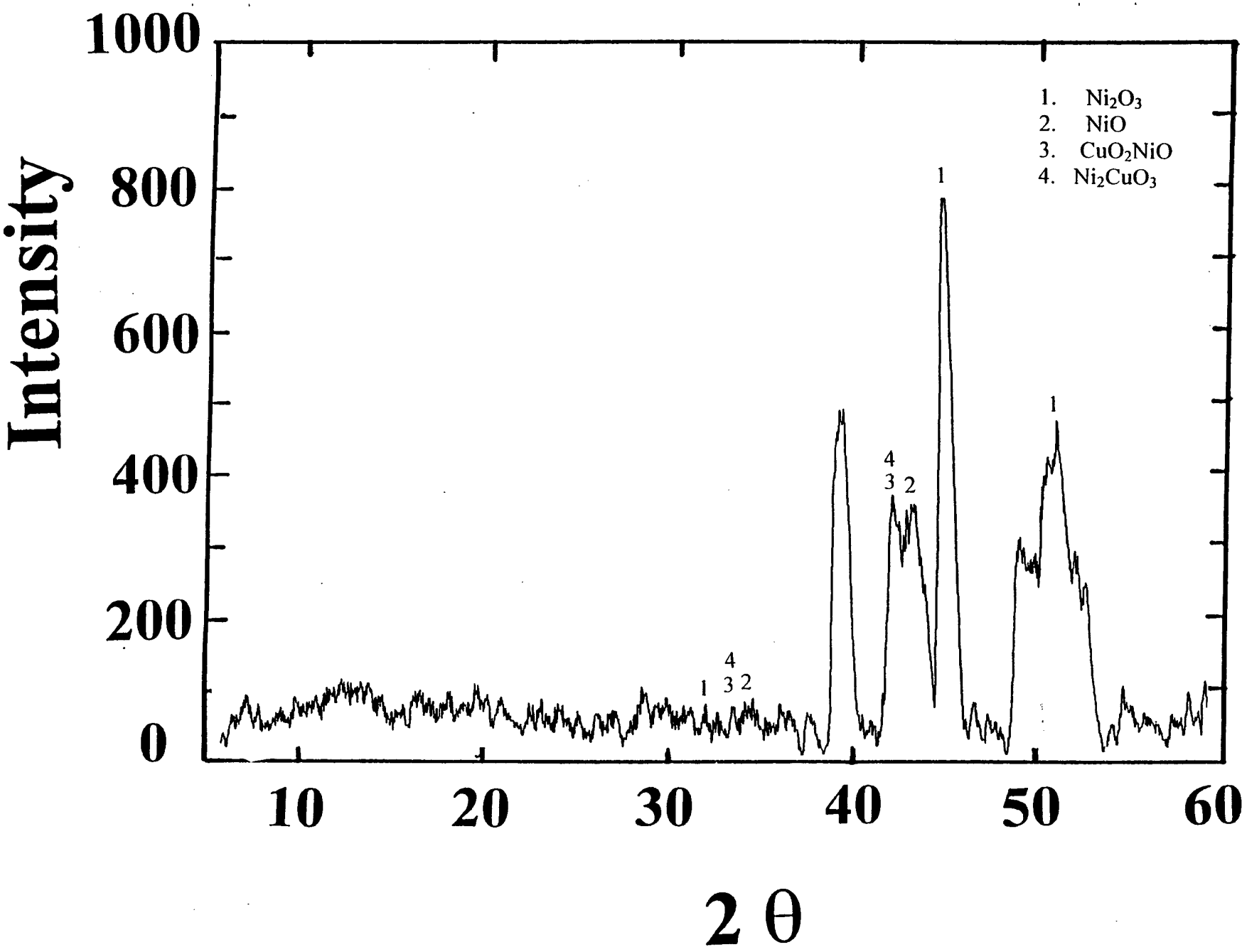

Figure 23. In-situ x-ray diffraction pattern obtained for 12.5 μm (0.0005") thick 90 – 10 Cu – Ni foil mounted on the electrochemical test cell, after exposure for 24 hours at + 0.1 V versus a Ni/NiO electrode.

XPS RESULTS FOR POTENTIALS OF + 500 mV

Figures 24 - 26 show XPS spectra for copper, nickel and oxygen obtained from test foils after corrosion testing at + 0.5 V in KOH solution for 24 hours. The results for the electrochemical reaction of 90-10 Cu-Ni foil at + 0.5 V in KOH suggest that the copper close to the surface is chemically transformed to $Cu(OH)_2$ and CuO. The nickel close to the surface is chemically transformed into NiO and Ni_2O_3 and a small fraction of Ni was also transformed into $Ni(OH)_2$.

DISCUSSION

Based on classical electrochemical reaction mechanisms, it can be suggested that when a negative potential (- 500 mV or – 100 mV) is applied to nickel and copper, the electrochemical cathodic reaction will proceed. The metals nickel and copper will be reduced to form $Ni(OH)_2$ and $Cu(OH)_2$ and other hydroxides with Ni^{+2} and Cu^{+2} states. Furthermore, at these negative potentials, the conversion of Ni^{+2} to a Ni^{+3} state and/or the formation of metal oxides ($Ni^{+3}OOH$, $Ni^{+3}{}_2O_3$, $Cu^{+2}O.Ni^{+2}O$) are not anticipated.

Similarly, when a positive potential is applied (+ 500 mV or + 100 mV) to nickel and copper, the electrochemical anodic reaction should proceed. The metals nickel and copper and their hydroxides (viz. $Ni(OH)_2$ and $Cu(OH)_2$) will be oxidized to form hydroxides and or oxides ($Ni^{+3}OOH$, $Ni^{+3}{}_2O_3$, $Ni^{+2}O$, $Cu^{+2}O$) with Ni^{+3} and Cu^{+2} state.

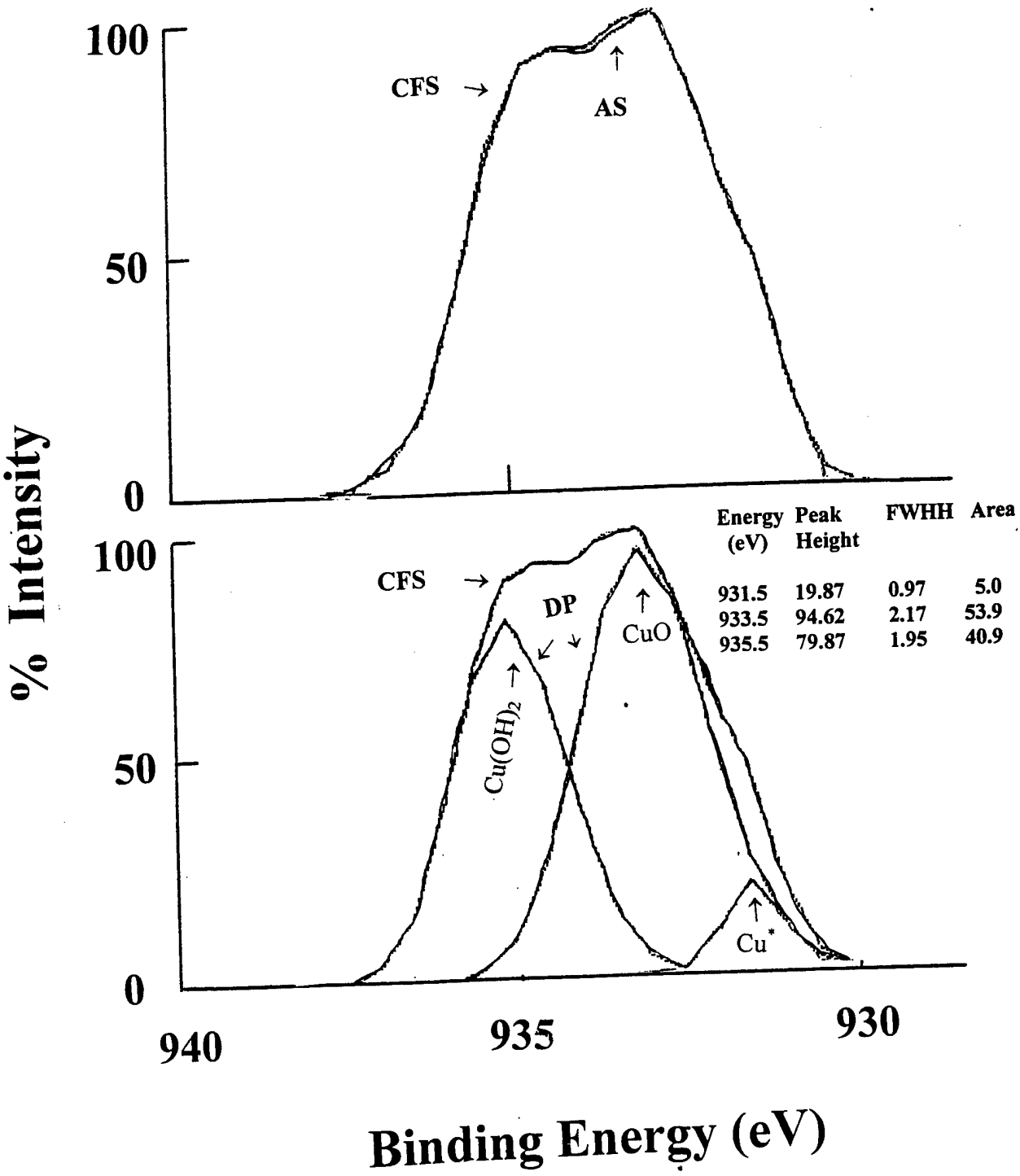

AS → **Actual XPS spectra**
CFS → **Copy of the XPS spectra generated by curve fitting**
DP → **De convoluted peaks of the curve fitted XPS spectra**
FWHH → **Full width half height**

Figure 24. Copper peaks obtained from XPS analysis of 12.5 μm (0.0005") thick 90-10 Cu-Ni foil surface exposed to the KOH at +0.5 V for 24 hours.

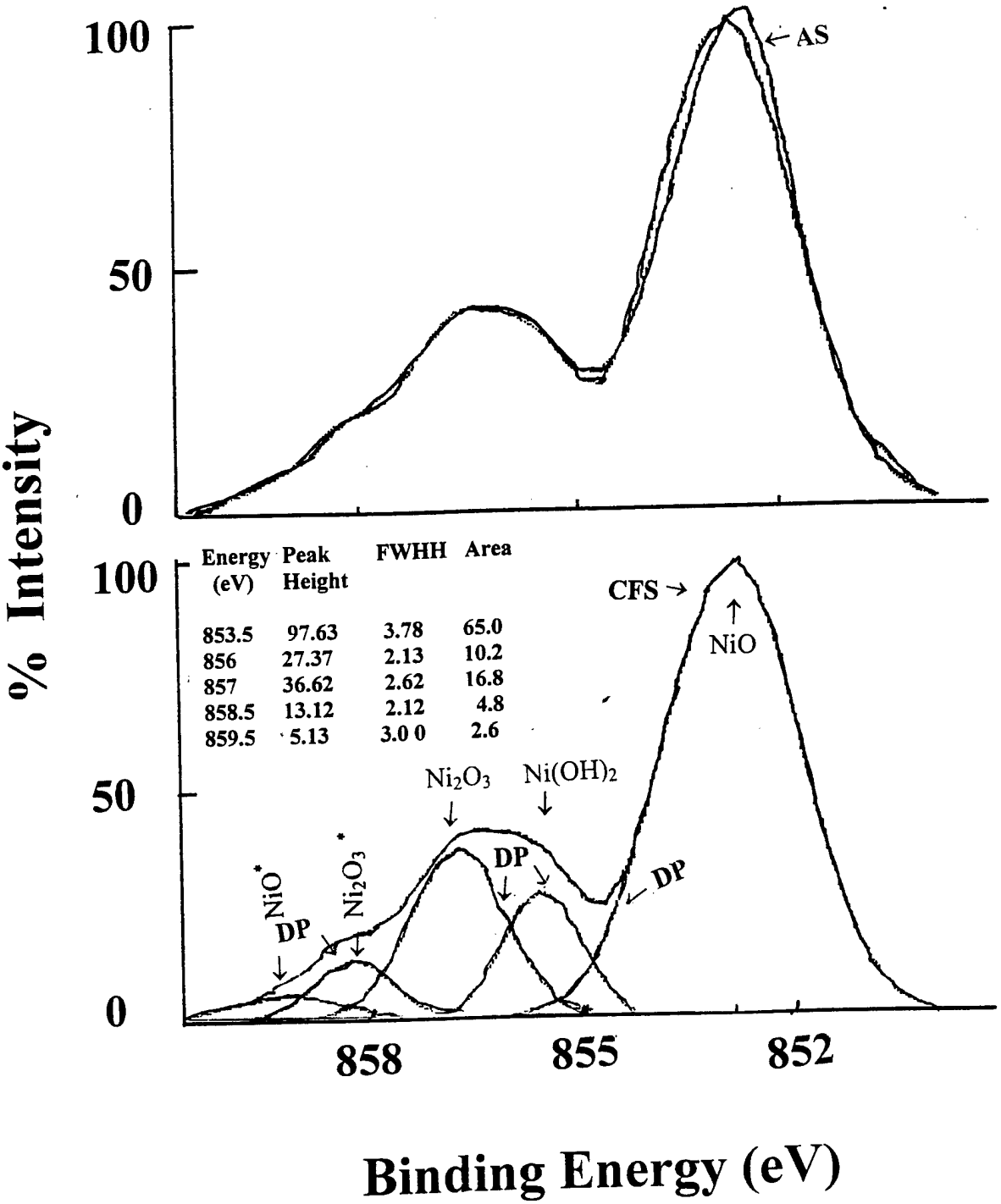

AS → Actual XPS spectra
CFS → Copy of the XPS spectra generated by curve fitting
DP → De convoluted peaks of the curve fitted XPS spectra
FWHH → Full width half height
* → Satellite or Minor Peak

Figure 25. Nickel peaks obtained from XPS analysis of 12.5 μm (0.0005") thick 90-10 Cu-Ni foil surface exposed to the KOH at +0.5 V for 24 hours.

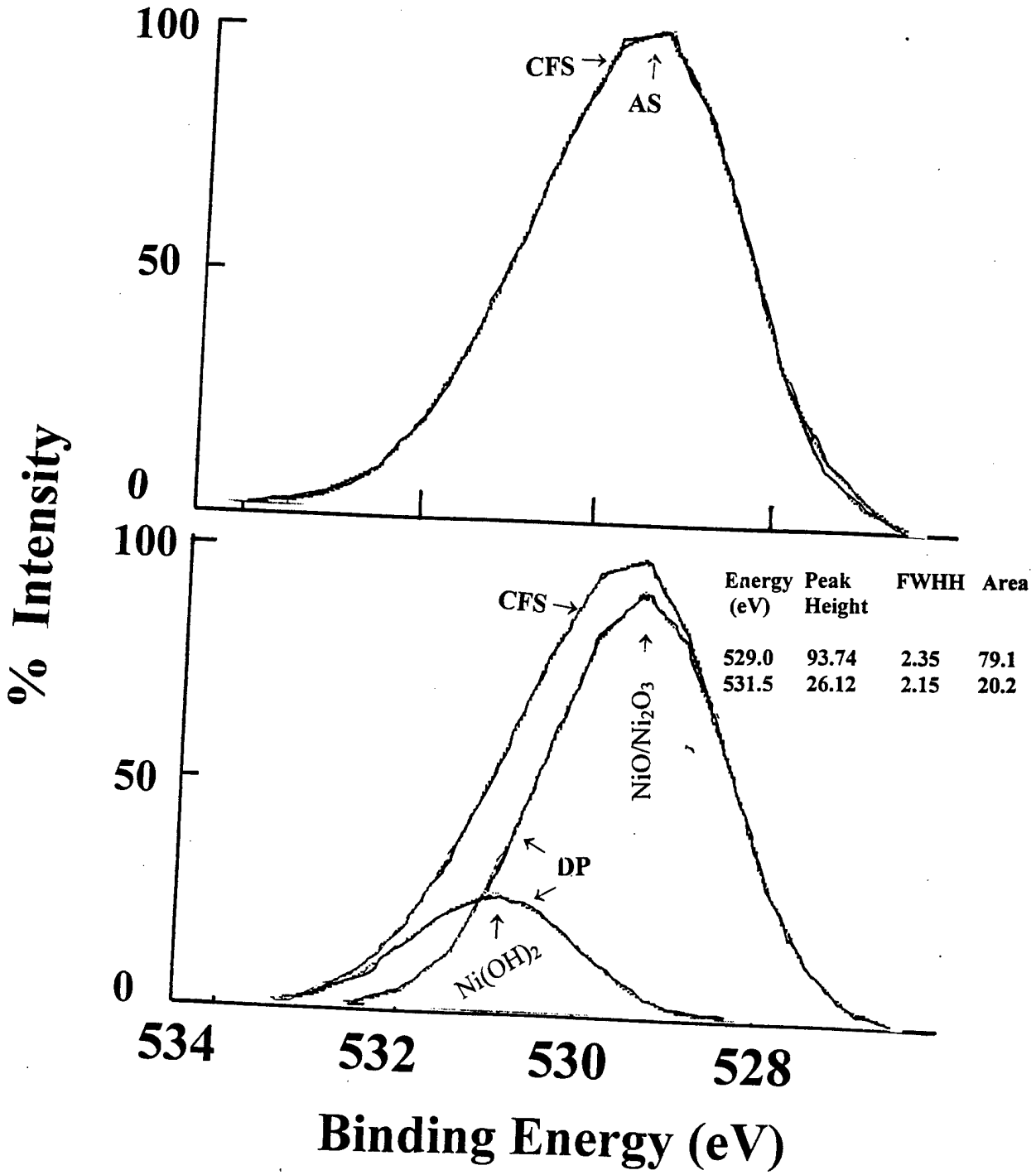

AS → **Actual XPS spectra**
CFS → **Copy of the XPS spectra generated by curve fitting**
DP → **De convoluted peaks of the curve fitted XPS spectra**
FWHH → **Full width half height**

Figure 26. Oxygen peaks obtained from XPS analysis of 12.5 μm (0.0005") thick 90-10 Cu-Ni foil surface exposed to the KOH at +0.5 V for 24 hours.

The present XRD results suggest that when – 500 and – 100 mV were applied, the 90-10 Cu-Ni alloy structure shows that in addition to the presence of $Ni(OH)_2$ and $Cu(OH)_2$, significant NiOOH and CuO phases were present. The XPS results indicate that at the 90 –10 Cu –Ni / KOH interface the outer alloy layers that are in contact with the KOH are transformed into $Ni(OH)_2$ and $Cu(OH)_2$. Therefore is possible that NiOOH and CuO phases are present as the inner passive layer of the alloy.

The XRD results suggest that when + 500 and + 100 mV were applied, the 90-10 Cu-Ni alloy structure shows the presence of some $Ni(OH)_2$ and $Cu(OH)_2$ and significant $Ni^{+3}{}_2O_3$, $Ni^{+2}O$, $Cu^{+2}O$ and potassium cuprates (with Ni^{+3} and Cu^{+2} states). The XPS results indicate that at the 90 –10 Cu –Ni / KOH interface the outer alloy layers that are in contact with the KOH are transformed into $Ni^{+2}(OH)_2$, $Ni^{+3}{}_2O_3$, $Ni^{+2}O$, $Cu(OH)_2$ and $Cu^{+2}O$ (with Ni^{+3} and Cu^{+2} states). Therefore, it is possible that $Ni^{+3}{}_2O_3$, $Ni^{+2}O$, and $Cu^{+2}O$ (with Ni^{+3} and Cu^{+2} state) phases are present as the inner passive layer of the alloy.

SUMMARY AND CONCLUSION

From the present investigation, the following conclusions can be made.

1. During the electrochemical reaction of the 90-10 Cu-Ni/KOH system, at - 0.5 V, significant $Ni(OH)_2$, NiOOH, $Cu(OH)_2$, $Cu^{+1}{}_2O.Ni^{+2}O$ and CuO are formed at the interface of the 90-10 Cu-Ni foil and the KOH solution.
2. From XRD and XPS analysis of the structure of the interface, it is possible to suggest that at – 0.5 V, both $Ni(OH)_2$,$Cu(OH)_2$ and CuO are present at the outer passive layer and NiOOH and $Cu^{+1}{}_2O.Ni^{+2}O$ are present at the inner passive layer.

3. At + 0.5 V, the interface (inner and outer passive layers) structure of the 90-10 Cu-Ni foil and the KOH solution consists of NiO, Ni_2O_3, Ni_2CuO_3, $Ni(OH)_2$, NiOOH, $Cu^{+1}{}_2O.Ni^{+2}O$ and CuO.

4. From XRD and XPS analysis of the structure of the interface, it is possible to suggest that at + 500 mV, the outer passive layer is comprised of NiO, Ni_2O_3, $Ni(OH)_2$, CuO and $Cu(OH)_2$ and the inner passive layer is comprised of $Ni(OH)_2$ and CuO.

ACKNOWLEDGEMENT

The author acknowledges the usage of the x-ray diffraction unit purchased by the Geology Department of the George Washington University under an NSF grant to Prof. Fred Siegel. The author would like to thank Prof. C. Gilmore of the Institute of Materials Science, George Washington University for permitting us to conduct experiments in his thin film laboratory. The author thanks Mr. Paul Goldy of the thin film laboratory of the Institute of Materials Science, George Washington University for his help in conducting experiments with the x-ray diffraction unit and for the operation of the XPS unit.

REFERENCES

1. Ross, P. N., and Wagner, F. T., "The Application of Surface Physics Techniques to the Study of Electrochemical Systems," Advances in Electrochem., 13, 69(1985).

2. Flischmann, M. and Hill, I. R., "Surface Enhanced Raman Spectroscopy," edt. Chang, R. K. and Furtak, T. 5., Plenum Pub., New York, 275 (1982).

3 Bewick, A. and Pons, B. S., "Advances in Infra-red and Raman Spectroscopy," edt. Clark, R. J. H., and Hester, RE., Pub., Wiley Heydon, New York 12, Chap. 1(1985).

4. Bomchil, O., and Rekel, C., " Neutron Diffraction Study of the Electrochemical Passivation of Nickel Powder," Electro Anal. chem., 101, 133(1979).

5. Lang, G. G., Kruger, J., Black, D. R. and Kuriyama, M., "Structure of Passive Films on Iron Using a New Surface–EXAFS Technique," J. Electrochem. Soc., 130, 240 (1983).

6. Bosio, L., Cones, R. and Froment, M., "Reflection EXAFS Studies of Protective Oxide Formation on Metal Surfaces," Proc. 3rd Int. EXAFS Conf., Stanford, CA (1984).

7. Marra, W. C., Elsenberger, P. and Cho, A. Y., J., " x-ray Total – External – Reflection – Bragg Diffraction: A Structural Study of Gallium Arsenide – Aluminum Interface," Appl. Phys, 50, 6927(1979).

8. Cowan, P. L., Goloychenko, J. A. and Robbins, M.F., " x- Ray Standing Waves at the Crystal Surface," Phys. Rev. Lett., 44, 1680 (1980).

9. Golovchenko, J. A., Patel, S. W, Kaplan, D. R., Cowan, P. L., and Bedzyk, P., "Solution to the Surface Registration Problem Using x- Ray Standing Waves," Phys. Rev. Lett., 49, 560(1982).

10. Pandya, K. I., O'Grady, W. E.Corrigan, D. A., Mc Breen, J. and Hoffman, R. W., " In – situ x – Ray Adsorption Spectroscopic Studies of Nickel Oxide Electrodes," J. Phys. Chem, 94, 21(1990)).

11. Rommel, H. E.G., "Time Dependent Energy Efficiency Losses at Nickel Cathodes in Alkaline Water Electrolysis Systems," MS Thesis, Johns Hopkins University, Baltimore, MD 1982.

12. Moran, P. J., and Guanti, R. S., "Measurement of Electrolyte Conductivity in Highly Conducting Solutions," 161st Electrochem. Soc., Meeting, Montreal, Canada, 1982.

13. Srinivasa Rao, A. and Murray. J. N, "Characterization of Surface Film Growth During the Electrochemical Process: Part I," NSWC CD –TR–61-98–17, June 1998.

14. Wagner, C. D., Riggs, W. M., Davis, L. E., Moulder, J. F. and Muilenberg, G. E., "Handbook of X-Ray Photoelectron Spectroscopy," Pub. By Perkin-Elmer Corp., Eden Prairie, MN (1979).

Distribution

	Copies
DEFENSE TECHNICAL INFORMATION CENTER 8725 JOHN KINGMAN ROAD SUITE 0944 FORT BELVOIR VA 22060-6218	1
ATTN LARRY J NELSON ELECTRIC POWER RESEARCH INSTITUTE 3412 HILLVIEW AVE PALO ALTO, CA 94304	1

INTERNAL DISTRIBUTION		*Copies*
CODE 0113	(DOUGLAS)	1
CODE 60	(WACKER)	1
CODE 61	(HOLSBERG)	1
CODE 612	(APRIGLIANO)	1
CODE 613	(FERRARA	1
CODE 613	(MURRAY)	1
CODE 613	(RAO)	5
CODE 614	(MONTEMARANO)	1
CODE 615	(DENALE)	1
CODE 3442	(TIC)	1